





Review

# State of the Art of Boron and Tin Complexes in Second- and Third-Order Nonlinear Optics §

Cristina C. Jiménez <sup>1</sup>, Alejandro Enríquez-Cabrera <sup>1</sup>, Oscar González-Antonio <sup>1</sup>,  
Javier Ordóñez-Hernández <sup>1</sup>, Pascal G. Lacroix <sup>2</sup>, Pablo Labra-Vázquez <sup>1</sup>, Norberto Farfán <sup>1</sup>  
and Rosa Santillan <sup>3,\*</sup>

<sup>1</sup> Facultad de Química, Departamento de Química Orgánica, Universidad Nacional Autónoma de México, Ciudad Universitaria, 04510 Ciudad de México, México; jimenezcuriel@yahoo.com (C.C.J.); enriquez\_ale@hotmail.com (A.E.-C.); freewheelin34@hotmail.com (O.G.-A.);

sogma\_javi@hotmail.com (J.O.-H.); pab.labra@gmail.com (P.L.-V.); norberto.farfán@gmail.com (N.F.)

<sup>2</sup> Laboratoire de Chimie de Coordination du CNRS, 205 route de Narbonne, F-31077 Toulouse, France; pascal.lacroix@lcc-toulouse.fr

<sup>3</sup> Departamento de Química, Centro de Investigación y de Estudios Avanzados del IPN, CINVESTAV, Apdo. Postal 14-740, 07000 Ciudad de México, México

\* Correspondence: rsantill@cinvestav.mx; Tel.: +52-555-747-3725

Received: 31 October 2018; Accepted: 5 December 2018; Published: 10 December 2018



**Abstract:** Boron and tin complexes have been a versatile and very interesting scaffold for the design of nonlinear optical (NLO) chromophores. In this paper we present a wide range of reports since the 1990s to date, which include second-order (e.g., second harmonic generation) and third-order (e.g., two-photon absorption) NLO properties. After a short introduction on the origin of the NLO response in molecules, the different features associated with the introduction of these inorganic motifs in the organic-based NLO materials are discussed: Their effect on the accepting/donating capabilities of the substituents, on the efficiency of the  $\pi$ -conjugated linkage, and on the topology of the chromophores which can be tuned from the first generation of “push-pull” chromophores to more sophisticated two- or three-dimensional architectures.

**Keywords:** organoboron complex; organotin complex; nonlinear optics; two-photon absorption; Second-Harmonic Generation

## 1. Introduction

Nonlinear optics is the multidisciplinary research domain which investigates the properties arising from the interactions of matter with intense electromagnetic fields, thus producing modified fields that are different from those of the input field in frequency, amplitude, phase or polarization [1]. Most nonlinear optical (NLO) responses were not observed before 1960 when Maiman built the first laser at the Hughes Research Laboratories of the Hughes Aircraft company in Malibu, California [2,3]. Since that time, the world of nonlinear optics is indeed intricately associated to the world of lasers.

In the summer of 1961, Peter Franken and his group [4], at the University of Michigan, at Ann Arbor performed the first experiment of frequency doubling, or Second Harmonic Generation (SHG), on a crystal of quartz irradiated by a ruby laser operating at 694 nm [5]. This first historical experiment is illustrated in Figure 1.

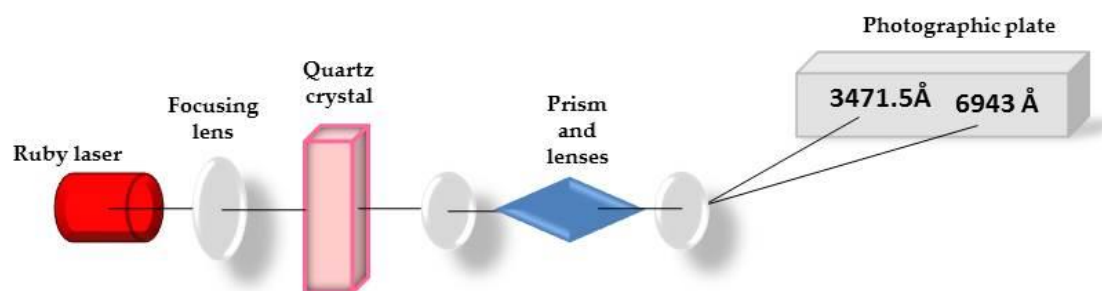


Figure 1. First observation of the second harmonic generation.

### 1.1. Organic Molecules for Second-Order NLO Properties

The first observation of a second-order NLO property in an organic material, was made by Rentzepis and Pao, at Bell Telephone Laboratories in 1964 [6], when crystals of 3,4-benzopyrene, and 1,2-benzanthracene were irradiated with intense ruby laser light. Later on, in 1978, Buckingham and Clarke [7], studied the NLO processes in atoms and molecules.

Since this pioneering work, organic materials have acquired relevance as they were found to exhibit ultra-fast response times to optical excitation, low dielectric constants and a synthetic design flexibility which allows to perform structural modifications to modulate the NLO effect, by virtue of the tremendous capabilities of organic synthetic chemistry [8]. Other advantages are their high optical damage threshold and low cost [1].

At the most fundamental level, the molecular NLO response is expressed from the polarization ( $\mu$ ) of a molecule subjected to a laser light as follows:

$$\mu(E) = \mu_0 + \alpha E + \beta E^2 + \gamma E^3 + \dots \quad (1)$$

An expression in which  $\mu_0$  is the permanent dipole moment,  $\alpha$  the polarizability,  $\beta$  and  $\gamma$  respectively the first- and second-order hyperpolarizabilities (origin of the first- and second-order NLO properties) and  $E$  being the electric field component of the light. The most investigated NLO properties (e.g., SHG) are ultimately related to  $\beta$  which is expressed in  $\text{cm}^5 \times \text{esu}^{-1}$ , which will be called esu here for simplification.

Although organic molecules with second-order NLO properties are only a class of NLO materials, they have dominated the field as the most studied chromophores. Furthermore, the electronic features required to understand the origin of their NLO response can easily be transposed to more sophisticated systems to a large extent. Therefore, they are described here as the most useful benchmark model for providing an efficient guideline towards the most promising NLO molecules.

Most traditional organic NLO chromophores are planar molecules with a strong electron-donating group (D) and an electron-acceptor group (A), connected via a  $\pi$ -conjugated structure acting as an electronic bridge to facilitate charge transfer across the molecule. These donor-acceptor chromophores are known as the “push-pull” systems (Figure 2).



Figure 2. “Push-pull” system.

The electron donor groups often have electron lone pairs of high energy and are characterized by hybridization with predominantly p characters ( $\text{sp}^3$ , 75% p), as in a disubstituted amine  $-\text{NR}_2$ . The electron acceptor groups (A) are characterized by the presence of unoccupied orbitals having low energy levels (as in three-coordinated boron compounds), with more s character bonding such as  $\text{sp}$  in nitrile, or  $\text{sp}^2$  in nitrobenzene organic compounds.

In 1968, Kurtz and Perry [9] described a simple and quick experimental technique which permits the rapid classification of materials according to a magnitude of nonlinear optical coefficients relative to a crystalline quartz standard, and the existence or absence of phase matching direction(s) for second-harmonic generation. The technique only requires the material in powder form (readily available in most cases), unlike single crystals of reasonably good optical and dielectric quality which are difficult to obtain. This development was the first systematic investigation for detecting second-harmonic generation in crystalline powders. With a reasonably high reliability, the method enables one to classify a new material in one of five categories: Class A: Phase-matchable for second-harmonic generation; nonlinear coefficients large (substantially greater than crystalline quartz), Class B: Phase-matchable for second-harmonic generation; nonlinear coefficients small (same order of magnitude as crystalline quartz), Class C: Nonlinear coefficients greater than crystalline quartz; not phase-matchable for second-harmonic generation, Class D: Nonlinear coefficients equal to or less than crystalline quartz; not phase-matchable for second-harmonic generation, and Class E: Centrosymmetric (first-order nonlinearities vanish due to symmetry considerations).

Kurtz and Perry provided an initial survey of approximately 100 compounds, SHG was detected for the first time in 56 of these materials and 27 of them were assigned to the phase-matchable categories. Single-crystal measurements on four of these latter compounds verified the existence of phase-matching directions for second-harmonic generation. This powder technique provided a substantial increase in the number of new materials for use in nonlinear optics applications.

In 1977, Oudar [10] reported the influence of donor and acceptor groups on the second and third order hyperpolarizabilities of a series of  $\pi$  conjugated molecules such as styrene and stilbene derivatives with various substituents. These were measured by static-electric field induced second harmonic generation (DC-SHG) and tunable four-wave mixing both in liquids and solutions. These compounds showed nonlinearities 10 times larger than their benzene derivatives, this is due to a greater  $\pi$  conjugated system. In the case of the disubstituted molecules containing donor and acceptor groups at opposite ends, they possess strong intramolecular charge transfer that promotes a large enhancement of  $\beta$ .

Among the numerous factors that contribute to the increase of second-order NLO properties in organic compounds are:

1. The relative position of the donor-acceptor groups on a  $\pi$ -conjugated structure in order to benefit from the best path of delocalization. For instance, in the example of a D/A disubstituted phenyl (Figure 3), it has long been recognized that the *para* substituted isomer leads to the best charge transfer effect and hence to the largest  $\beta$  value.
2. The length of the  $\pi$  system. Increasing the length of the  $\pi$  system increases the NLO properties of organic compounds, since the long range  $\pi$ -delocalization brings the main component to the molecular polarizability (Equation (1)). In high- $\beta$  chromophores, computations based on the Pariser-Parr-Pople (PPP) model have proven useful and reliable when applied to different chromophores. Experimentally-determined  $\beta$  values and PPP-obtained show an excellent correlation ( $\beta_{\text{PPP}} \leq 2.5 \beta_{\text{exp}}$ ), the largest value has been achieved by **C7**  $\beta_{\text{vec}}^{(\text{PPP})} = 466.8 \times 10^{-30}$  esu and  $\beta_{\text{vec}}^{(\text{exp})} = 470 - 790 \times 10^{-30}$  esu. (Figure 4) [11,12].
3. Crystallization in non-centrosymmetric space groups in the case of second-order bulk effects. Equation (1) leads to the important symmetry requirement that, in order for  $\beta$  to be non-zero, the molecule must necessarily be non-centrosymmetric. This can be easily understood from the fact that  $\mu(-E) = -\mu(E)$  in centrosymmetric entities, therefore  $\beta(-E)(-E) = \beta(E)(E)$  and hence  $\beta = 0$ . The polarization (P) of a macroscopic material is again given by an expression analogous to Equation (1), expressed as follows:

$$P(E) = \chi^{(0)} + \chi^{(1)}E + \chi^{(2)}E^2 + \chi^{(3)}E^3 + \dots \quad (2)$$

where  $\chi^{(2)}$  is the second-order susceptibility which is related to the underlying  $\beta$ . An important point to note is that the requirement for non-centrosymmetry is valid in the solid state as well,

so the molecules must necessarily crystallize in non-centrosymmetric space groups. In that case, the bulk property is frequently approached semi-quantitatively through a solid state powder test which expresses the SHG efficiency of the materials versus that of a reference (e.g., urea [13]). Some examples of organic solids with SHG efficiencies are gathered in Figure 5 [14].

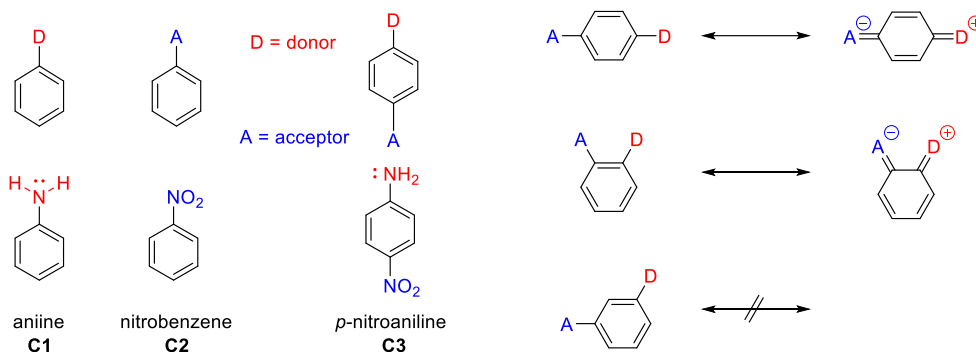


**Figure 3.** The relative position of the donor–acceptor groups.

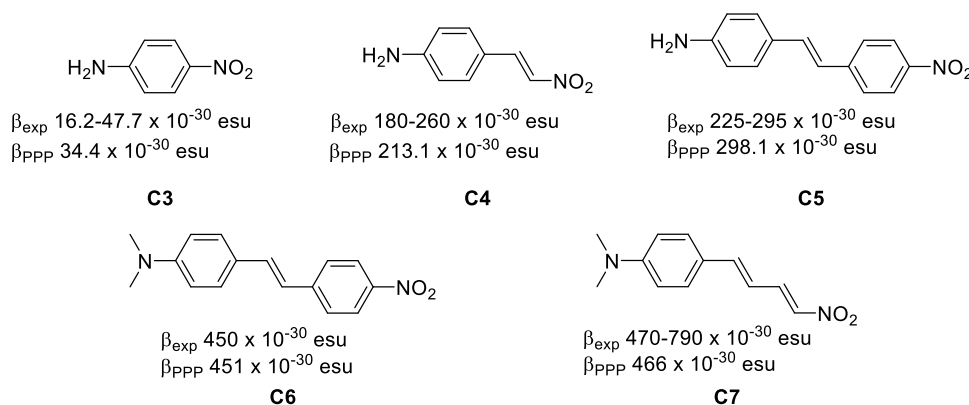


**Figure 4.** The effect of the length of the  $\pi$  system on the first-order hyperpolarizability.

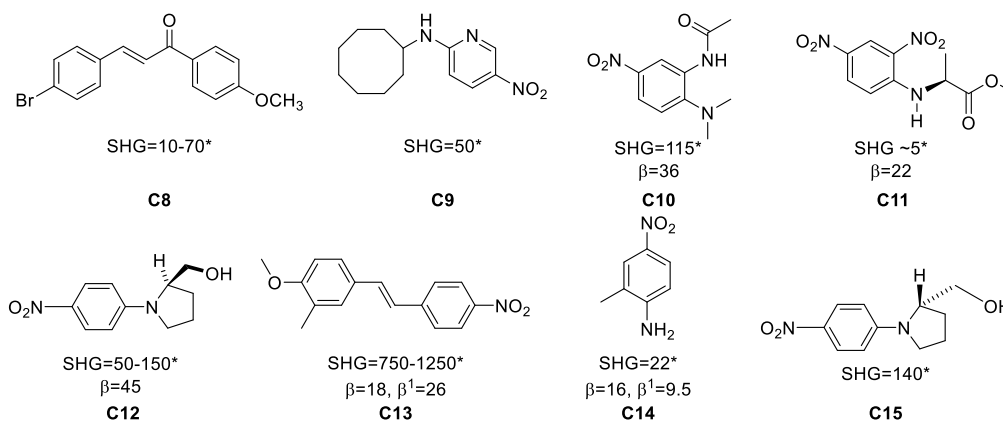


**Figure 5.** Examples of organic materials that have been studied as single crystals for frequency doubling.

\* Powder Second Harmonic Generation (SHG) vs. urea;  $\beta$  in  $\times 10^{-30}$  esu at 1.06  $\mu\text{m}$ ;  $\beta^1$ : at 1.9  $\mu\text{m}$ .

Thus, the reported powder SHG value for the series of compounds **C8–C15** in Figure 5 are some noteworthy cases in terms of their SHG values. For instance, 4-bromo-4'-methoxychalcone, (**C8**), shows  $\beta$  values of 10–70 *vs.* urea, depending on the solvent from which the material was crystallized, for 2-*N*-cyclooctylamino-5-nitropyridine (**C9**)  $\beta = 50$  *vs.* urea while 3-methyl-4-methoxy-4'-nitrostilbene (**C13**) has the highest reported  $\beta$  value, 1250 times *vs.* urea, and 2-methyl-4-nitroaniline (**C14**) shows a value of 22 *vs.* urea.

### 1.2. From Second-Order to Third-Order NLO Properties

At first, the key parameters at the origin of the third-order properties ( $\gamma$  in Equation (1)) seem to be closely related to those at the origin of  $\beta$ , making the third-order properties a simple extension of the second-order properties. On the other hand,  $\gamma$  is related to an odd term ( $\propto E^3$ ) in the development of Equation (1), therefore it is subject to no symmetry requirement. Indeed, centrosymmetric molecules, which are silent in second-order nonlinear optics, can be strongly efficient in third-order applications. Moreover, it has been suggested by Marder [15] that the most promising strategy to optimize  $\gamma$  should be to focus the search on chromophores having a vanishing  $\beta$ . Along this line, the most efficient systems in third-order nonlinear optics should necessarily be centrosymmetric. Therefore, there are two classes of efficient third-order chromophores: The dipolar (“push-pull”) chromophores exhibiting both second- and third-order properties, and the quadrupolar (centrosymmetric) chromophores in which extremely large third-order NLO responses can be observed [15].

There are numerous optical properties associated to  $\gamma$  (e.g., third harmonic generation, Kerr effect) but the most widely investigated one is the capability for a molecule to absorb two photons simultaneously, known as two-photon absorption (TPA) [16]. While the capability of a molecule to absorb one photon is related to its extinction coefficient ( $\epsilon$ ), its capability to absorb two photons is quantified as the molecular cross-section ( $\sigma_{TPA}$ ) expressed in Göppert-Mayer (GM). In the present review, most of the third-order reports will be on the cross-section ( $\sigma_{TPA}$ ) rather than on the third-order hyperpolarizability  $\gamma$  however, they are related by the following expression:

$$\sigma_{TPA} = \frac{8\pi^2 \hbar \omega^2}{n^2 c^2} L^4 \text{Im}\gamma \quad (3)$$

where  $\omega$  is the laser frequency,  $n$  the refractive index,  $c$  the velocity of light in vacuum,  $L$  the local field factor, and  $\text{Im}\gamma$  the imaginary part of  $\gamma$  [16–18].

Finally, the choice to talk specifically about boron and tin complexes, from the myriad of inorganic NLO-responsive species, springs from three main points. First, as will be seen through the contents and as can be seen in the literature, there has been a perfectly traceable evolution in design and rational building of NLO-responsive chromophores that stems from the understanding of their electronic properties and synthetic accessibility. Therefore, it is possible to perform a historical tracing of the attempts to obtain better chromophores of this kind, that help to clarify fundamental phenomena and that can possess different applications. Secondly, in the recent years, there is no compendium about the species we will discuss further down in the present text. Due to the abundance of boron and tin complexes, review articles about modern architectures and applications are severely scarce and scattered in terms of the compounds they encompass. In the case of tin, this is even more evident since the available literature about tin complexes specifically as NLO-responsive species is not so abundant. So, our intention is to pursue a comprehensive compendium which deals with the modern literature about this important chromophores.

## 2. NLO Properties in Organoboron Compounds and Boron Complexes

### 2.1. Second-Order NLO Properties

Boron compounds that exhibit nonlinear optical properties can generally be found in three forms:

1. Where boron is in neutral form, it acts as electron acceptor due its Lewis acid character. This is exemplified in Figure 6 for 5-(dimesitylboryl)-5'-(pyrrolidin-1-yl)-2,2'-dithienyl **B1**.
2. Where boron is in ionic form, it acts as an electron donor, as observed in **B2** (Figure 8).
3. Where the boron forms an adduct with nitrogen, for instance in a boronated pyridine (Figure 7), the creation of the B–N bond turns the pyridine from a weak withdrawing unit to a much stronger one, which leads to enhanced intramolecular charge transfer and hence, larger NLO response.

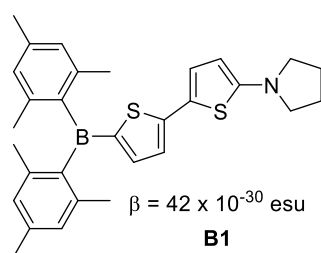


Figure 6. Boron in neutral form.

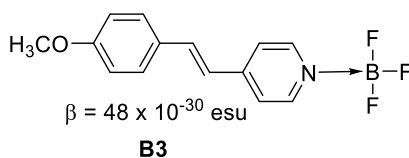


Figure 7. Boron forming an adduct with nitrogen.

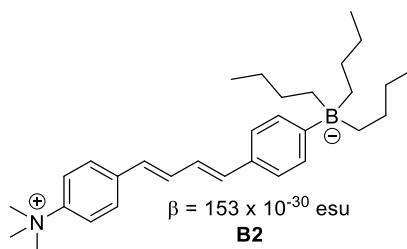


Figure 8. Boron in ionic form.

Various three-coordinated and tetracoordinated boron containing materials have been reported in relation to potential NLO properties.

The most characteristic electronic properties of trivalent boron are related to its vacant  $p_z$ -orbital [19] (Figure 9).

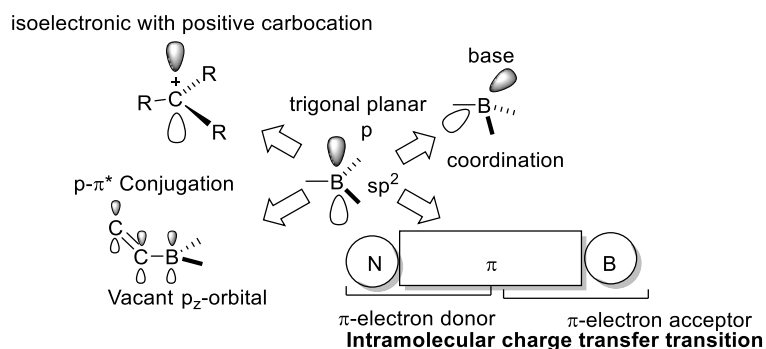


Figure 9. Main features of three-coordinated boron compounds.

Three-coordinated boron atom is an electron acceptor, it is a Lewis acid, and is isoelectronic to a carbocation; with a trigonal planar geometry, it is electron deficient, which allows an effective  $\pi$ - $p$  conjugation with an adjacent organic  $\pi$ -system. The Lewis acid character of three-coordinated boron atom can be inhibited by steric hindrance.

Tetracoordinated boron acts as an electron-donating substituent and possesses a negative charge and an occupied  $p_z$ -orbital. Tetracoordinated boron compounds are more stable than the three-coordinated ones, and the modification of the electronic and hindrance effects allows the tuning of their nonlinear optical properties.

The development of functional materials which use boron as the main element started with the work of Williams from the Kodak group [20,21]. Kanis et al. [11] made the first theoretical calculations of the quadratic hyperpolarizabilities of organoboranes in stilbene chromophores, in 1991 using the semiempirical ZINDO calculations.

Yuan, Marder et al. [22] synthesized air-stable “push-pull” E-alkenes of the form E-D-CH=CH-B(Mes)<sub>2</sub> by hydroboration of  $\pi$ -donor substituted alkynes with dimesitylborane as a  $\pi$ -electron acceptor, obtaining  $\beta$  values of  $11 \times 10^{-30}$  esu for 4-Me<sub>2</sub>N-C<sub>6</sub>H<sub>4</sub>-B(Mes)<sub>2</sub>, and  $9.2 \times 10^{-30}$  esu for 4-H<sub>2</sub>N-C<sub>6</sub>H<sub>4</sub>-NO<sub>2</sub>.

In 1991, Lequan et al. [23] evidenced large changes in dipole moment occurring upon charge transfer transitions through an investigation of the solvatochromic shift in the push-pull derivatives 4-(dimethylamino)biphenyl-4'-yl]dimesitylborane (**B4**) and [4-(dimethylamino)-phenylazophenyl-4'-yl]dimesitylborane (**B5**). Solvatochromism provides an approach towards  $\beta$ , based on a dominant charge transfer transition accounting for the entire NLO response of the molecule. Under this assumption, the so called resulting  $\beta_{CT}$  were found to be equal to 37 and  $210 \times 10^{-30}$  esu. (Figure 10).



Figure 10. Second order hyperpolarizabilities for **B4** and **B5**.

Later on, the  $\beta$  values of these two chromophores were estimated more accurately by use of the EFISH techniques [13,24] which allows to get the projection of  $\beta$  along the molecular dipole moment ( $\mu_0$ ) of the chromophores; assuming  $\beta$  parallel to  $\mu_0$  leads to the actual hyperpolarizability  $\beta$  value of  $42 \times 10^{-30}$  for **B4** and  $72 \times 10^{-30}$  esu for **B5** [14] were obtained. The sizeable NLO response indicates an excellent withdrawing capability of the dimethyl boron comparable to that of a nitro substituent.

In 1993, Yuan et al. [25] synthesized “push-pull” organoboranes (E)-Fc-CH=CH-B(Mes)<sub>2</sub> and (E)-Ph<sub>2</sub>-P-CH=CH-B(Mes)<sub>2</sub>, powder SHG signal was observed for the latter compound which crystallized in a non-centrosymmetric space group. Evaluation of  $\beta$  by the EFISH technique, resulted in a value of  $-24 \times 10^{-30}$  esu, comparable to many classical organic donor-acceptor systems.

In 1996, Branger et al. [26] synthesized molecules with dimesitylboron as the acceptor group, bithiophene as the unsaturated chain and pyrrolidine-1-yl, dithienylidene and 3-thienyl as donor groups. EFISH measurements revealed  $\beta$  values of  $37 \times 10^{-30}$  esu for **B6** and  $31 \times 10^{-30}$  esu for **B7** derivatives. The replacement of the biphenyl unsaturated chain by bithiophene improved the dipole moment and the quadratic hyperpolarizabilities of the boron derivatives, despite a lack of planarity suggested at the computational level (Figure 11).

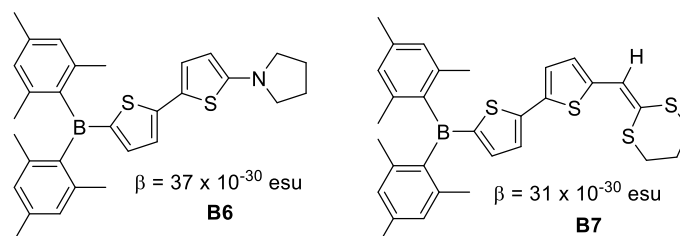
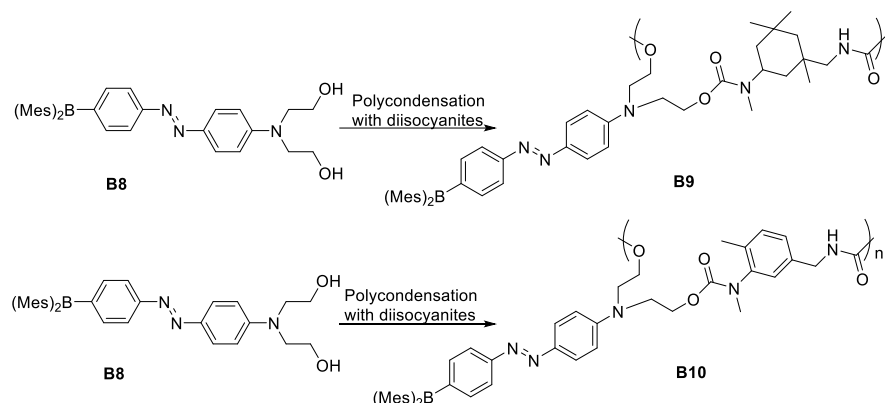


Figure 11. Hyperpolarizabilities for compounds with dimesitylboron as acceptor group, bithiophene as the unsaturated chain and as donor groups, pyrrolidine-1-yl and dithienylidene.

In 1997, Branger et al. [27] synthesized new polyurethanes with high glass transition temperature ( $T_g$ ) containing azo-dyes with NLO properties in which dimesityl boron groups are used as electron acceptors (Figure 12). Having high  $T_g$  polymers leads to the expectation that once aligned at high

temperature under strong electric fields, this will result in non-centrosymmetry, and therefore the NLO signal will be maintained at room temperature all over the life time of the device.



**Figure 12.** Polyurethanes having azo-dyes with a dimesityl boron group as an electron acceptor.

In 1998, Lesley et al. [28] reported on the second-order NLO properties determined by the EFISH technique in a series of neutral pyridyl adducts containing the strong Lewis acids  $BF_3$  and  $B(C_6F_5)_3$ . This study indicates that there is a good communication in chromophores with coordinated Lewis-acidic boranes,  $BF_3$  and  $B(C_6F_5)_3$ , acting as efficient electron acceptors. The  $\beta$  values range between  $48 \times 10^{-30}$  esu for **B11** and **B12** to  $155 \times 10^{-30}$  esu for **B14**. The  $\beta(0)$  values range between  $30 \times 10^{-30}$  esu to  $72.5 \times 10^{-30}$  esu for the pyridine/ $BF_3$  and  $B(C_6F_5)_3$  Lewis adducts. The  $\beta \times \mu$  product is doubled in most cases upon complexation with the strong Lewis acids, due to an increase of the molecular dipole moments ( $\mu$ ) and the second-order NLO coefficients ( $\beta$ ), the largest values being realized for the (dimethylamino)stilbazole derivatives. Finally, the NLO response is increased by 50% as compared to the disperse red 1 (DR1) standard reference (Figure 13).

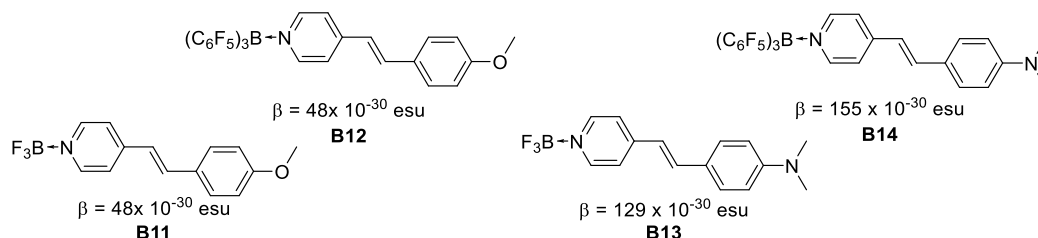


**Figure 13.** Binding Lewis-acidic boranes to stilbazoles.

Further computational investigations by Su et al. in 2001 [29] using the quantum chemical AM1/Finite Field method on pyridine, styryl pyridine, and phenylethynyl pyridine/borane adducts were in good agreement with the experimental values determined by Lesley [28].

In 2002, Farfán, Santillan, Lacroix et al. [30] studied "push-pull" boronates, in which the boron atom is attached in the  $\pi$ -conjugated bridge. They observed that  $\beta$  may be influenced by the molecular geometry in the vicinity of the boron atom. A computational investigation revealed that tuning the hyperpolarizability becomes possible by a controlled rotation of the phenylboronic fragment (Figure 14).

In 2002, Entwistle and Marder [31] reviewed the nonlinear optical properties of three and four-coordinate boron (which have been discussed before in this manuscript), and related compounds and polymers, highlighting the contributions of Williams, Glowgowski, Kaim, Lequan, and Marder groups.

In 2004, Entwistle and Marder [32] studied  $\beta$  by the EFISH technique for 4,4'-(dimesitylboryl)(*N,N*-dimethylamino)stilbene, which was found to be  $45 \times 10^{-30}$  esu at  $1.907 \mu m$ .

In 2006, Yamaguchi and Wakamiya [33] discussed the characteristic features of the boron element that their group use as a basis of molecular design. This is based on three fundamental features of

the boron element: (1) The existence of an empty p-orbital; (2) the Lewis acidity of boron; and (3) the geometric feature of boron.

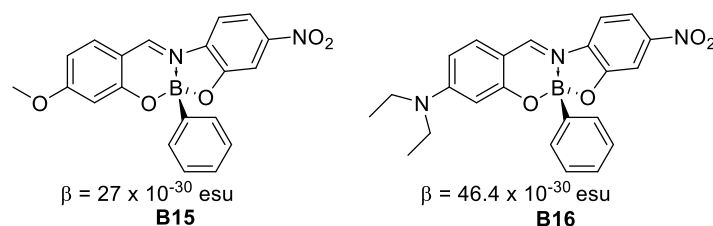


Figure 14. “Push-pull” boronates.

In 2006, Lamère, Farfán, Lacroix et al. [34] proposed a molecular switch induced by an electric field applied on a tetracoordinated boron compound, containing two “push-pull” units engineered with free rotation along the boron-carbon bond of a bisboronate structure (Figure 15). The NLO response was compared with that obtained for the monomeric derivative, by the EFISH technique. While the ground state conformation (the off state) is centrosymmetric and SHG silent, the application of an external electric field gradually aligned the subunits and increases the NLO response of the molecule. The EFISH signal is 1.95 times larger for bisboronate than for its monoborated analogue.

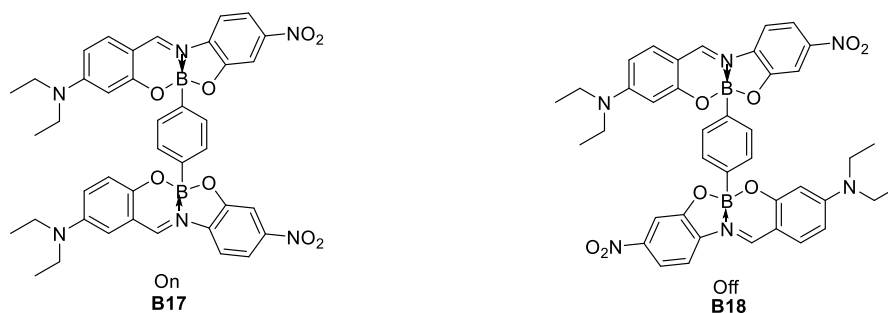


Figure 15. Molecular switch with NLO properties.

In 2008, Santillan et al. [35] found that boronates derived from Schiff bases present second (by EFISH technique) and third order NLO properties that could be tuned by modifying the conformations of the aryl fractions around the boron-carbon bonded to a naphthyl fragment (Figure 16).

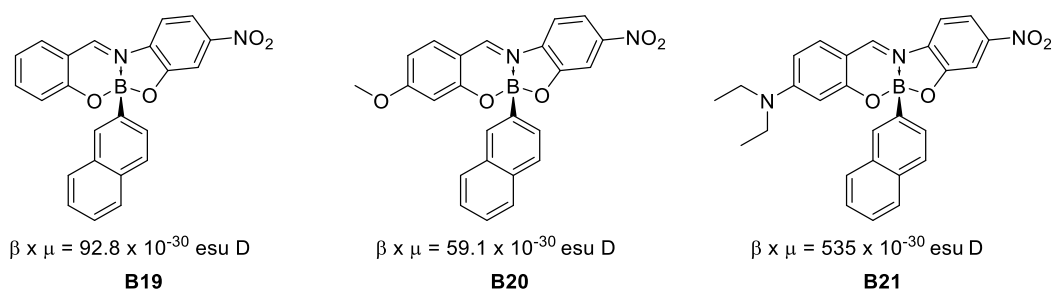
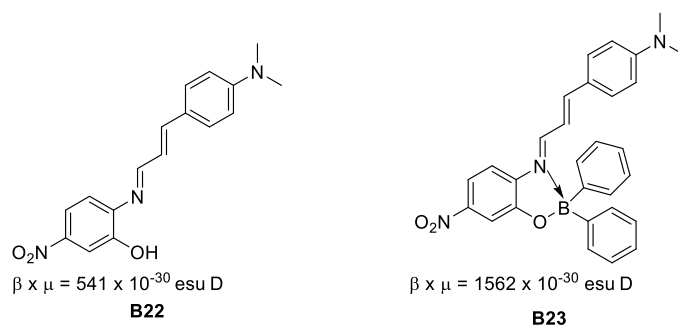


Figure 16. Schiff bases with second-order NLO properties.

In 2009, Lacroix, Farfán, Santillan et al. [36] reported on the synthesis of three boronates derived from bidentate imine ligands. The  $\beta \times \mu$  product recorded by EFISH shows a trend for a general increase of the NLO response after boron complexation (Figure 17).



**Figure 17.** Hyperpolarizability response after boron complexation.

Another synthetic effort undergone during 2015, was the one by Zhang [37], whose team modified the (Mes)<sub>2</sub>B (**B24**) group through substitution of the methyl groups of the boron atom by electron-withdrawing perfluorophenyl (**B25**) and 3,5-bis(trifluoromethyl)phenyl (**B26**) substituents, to produce the acceptor groups (2,6-Me<sub>2</sub>-4-C<sub>6</sub>F<sub>5</sub>-C<sub>6</sub>H<sub>2</sub>)<sub>2</sub>B ((Pfp)<sub>2</sub>B) and (2,6-Me<sub>2</sub>-4-(3,5(CF<sub>3</sub>)<sub>2</sub>-C<sub>6</sub>H<sub>3</sub>)-C<sub>6</sub>H<sub>2</sub>)<sub>2</sub>B ((Tfp)<sub>2</sub>B), respectively (Figure 18). Zhang found that tuning the donor strength by exchanging the triphenylamine donor for the stronger donor 1,1,7,7-tetramethyljulolidine (**B28** and **B29**) gave further fine control over the optoelectronic properties. Even if the NLO properties of these compounds have not been recorded, they could be considered as good candidates due to their architecture.

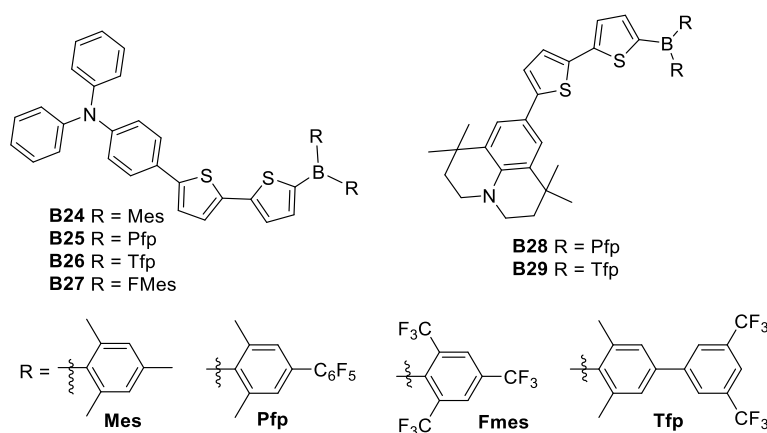


**Figure 18.** Substitution of the methyl substituents *para* to the boron atom by electron-withdrawing perfluorophenyl.

In 2017, Ji, Griesbeck and Marder [38] highlighted recent contributions using BMe<sub>2</sub> moieties along with the development of alternative strong B-based  $\pi$ -acceptors, focusing on systems which retain or enhance the air-stability of such species, a property which is most desirable for ease of preparation and handling, and thus for use in electronic or optical devices, as well as other applications.

The above examples indicate that tri-coordinated and tetracoordinated boron compounds are promising materials for different NLO applications. The lack of stability presented by the three-coordinated compounds was surpassed by the introduction of bulky groups such as B(Mes)<sub>2</sub> groups.

In this revision we have not addressed the group of compounds based on boron clusters since a comprehensive analysis of their nonlinear properties are out of the scope of this review. The readers are referred to the work published by Gao and Hosmane [39] and Nuñez and co-workers [40] for excellent overviews on the topic. Instead we have selected two reports on metallocarboranes that describe the supramolecular structure and its relationship with NLO response.

In 2014, Ma and co-workers [41] reported a DFT analysis of how the redox-driven, switchable, rotatory movement of a series of nickel metallocarboranes can be regulated through second-order nonlinear optical properties. Figure 19 depicts graphically that the computed properties (axial rotation

energy, redox pair potential and second-order hyperpolarizability) are substituent dependent in such a way that when electron donation increases in the substituted boron vertexes, the energy required to rotate the metallacarborane portion decreases, the redox potential decreases also, and the second-order response increases (Table 1). This result provides a strong rational design for tuning and enhancing NLO properties in these species.

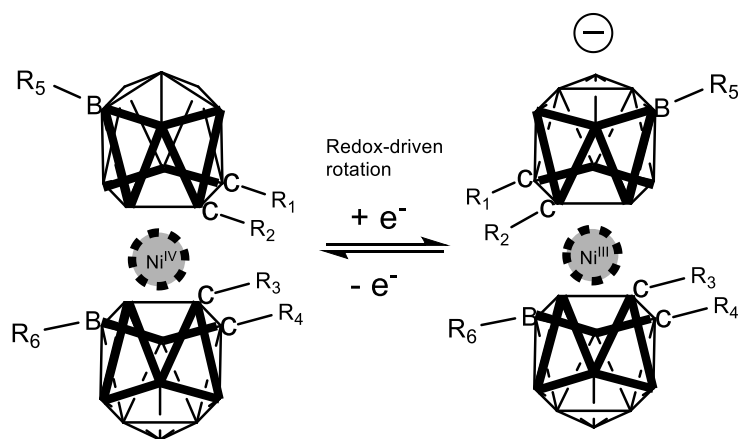


**Figure 19.** Computed properties of the rotational phenomenon of nickel-coordinated metallacarboranes, whose movement is redox- and NLO-dependent.

**Table 1.** Measured second-harmonic signals at 1.064  $\mu\text{m}$  and 1.907  $\mu\text{m}$  wavelengths relative to urea.

#	R <sub>1</sub>	R <sub>2</sub>	R <sub>3</sub>	R <sub>4</sub>	R <sub>5</sub>	R <sub>6</sub>	$\Delta G_{\text{rotation}}^a$	$E^{\circ}_{\text{redox}}^b$	$\beta$ (a.u.) <sup>c</sup>
B30	H	H	H	H	H	H	−111.877	0.13	163
B31	Me	Me	Me	Me	Me	Me	−113.874	0.22	120
B32	H	Ph	H	Ph	H	H	−118.474	0.42	1880
B33	H	Ph-OMe	H	Ph-OMe	H	H	−115.713	0.30	6674
B34 <sup>d</sup>	H	Ph-OMe	Ph-OMe	H	H	H	−112.701	0.17	4345
B35	H	H	H	H	Ph-OMe	Ph-OMe	−110.191	0.06	20998

<sup>a</sup> in kcal/mol; <sup>b</sup> in V; <sup>c</sup> computed for Ni(IV); <sup>d</sup>  $\beta$  was also computed for Ni(III) and it is 2903 a.u.

The interesting work by Gassin and collaborators [42] ponders on the close relationship between interfacial properties of dispersed systems and their potential NLO responsiveness. It is well known that a surfactant is an amphiphilic solute that at certain concentration stabilizes its content in solution by saturating the interphase between two media. Usually, when we refer to this kind of compound we talk about species with two clear portions differentiated by polarity (one portion being hydrophilic and polar, and the other portion of hydrophobic nature), although rare, there is the case of some cobalt metallacarboranes, which in neutral form possess no interfacial properties, but when deprotonated to the anionic form, they behave like surfactants. Knowing the surfactant-like behavior of the cobalt-coordinated dimetallacarborane (COSAN) anion (Figure 20), Gassin tested different solutions at concentrations of 0 mM, 0.06 M and 5.0 mM. SHG was measured in these solutions, varying the geometric dispositions of the fundamental frequency finding different second-order responses that depend on the orientation. This is indicative of a preferential supramolecular array, in which the COSAN anion molecules form a layer of axially arranged dimetallacarboranes. Adsorption isotherms determined for the COSAN solutions provided further insight on the interfacial arrangement, evidencing that certain axial anionic repulsion was taking place. With all these facts, it was proposed that the driving force for this supramolecular arrangement was the presence of dihydrogen bonds, as depicted in Figure 20. This study is an example of a somewhat overlooked application of NLO properties: The second-order response as means to elucidate structural problems of fundamental supramolecular chemistry.

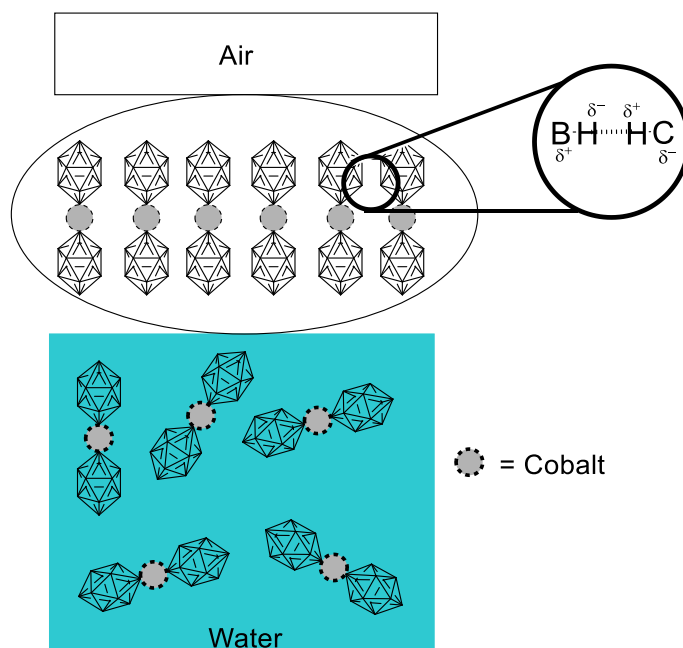


**Figure 20.** Schematic representation of the interfacial behavior and driving force for supramolecular arrangement of COSAN dimetallacarborane, measured primarily through second-order NLO response.

## 2.2. Third-Order NLO Properties

In the first half of 1990, boron compounds with NLO properties were studied carefully and systematically in terms of second-order hyperpolarizability ( $\beta$ ), to understand the correlation between electronic and NLO properties.

Concise examples of these discoveries were the electron-acceptor character of trivalent boron due to the presence of an empty p-orbital which, combined with a  $\pi$ -bridged structure having an electron-donating group, such as an amine, formed a dipolar “push-pull” architecture with important electronic communication along the structure [23,43], as depicted in Figure 21.

The other main design used for boron nonlinear optics resulted in what could be called an electronic *umpolung* [44], since the character of boron was reversed to be used as an electron-donor, rendering it tetravalent by adding an electron-accepting group. The design maintained a  $\pi$ -bridge of varying length [45], as shown in Figure 21.

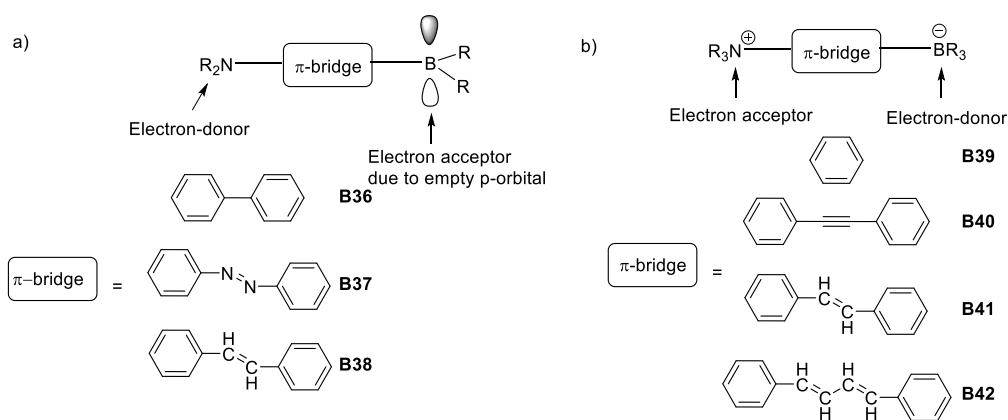


**Figure 21.** Boron-based architectures searched for NLO properties during the early 90s. (a) Dipolar design varying  $\pi$ -bridges with trivalent boron as electron acceptor unit; (b) dipolar architecture varying  $\pi$ -bridges with tetravalent boron as donor unit.

At the end of the 1990, TPA-responsive organic structures without boron were synthesized using two main designs: (1) A strong dipolar “push-pull” structure (as mentioned before) and (2) a quadrupolar structure to enhance TPA. Examples of these approaches can be found in the study reported by Reinhardt and co-workers [46] where both architectures were explored; using benzothiazole and substituted diphenylamines as electron-donor moieties, bi-thiophene and fluorene derivatives as  $\pi$ -bridges and a pyridine unit as the electron-acceptor (Figure 22). The only drawback is the modest  $\sigma$ TPA values which barely surpass 115 GM in contrast with the synthetic difficulty.

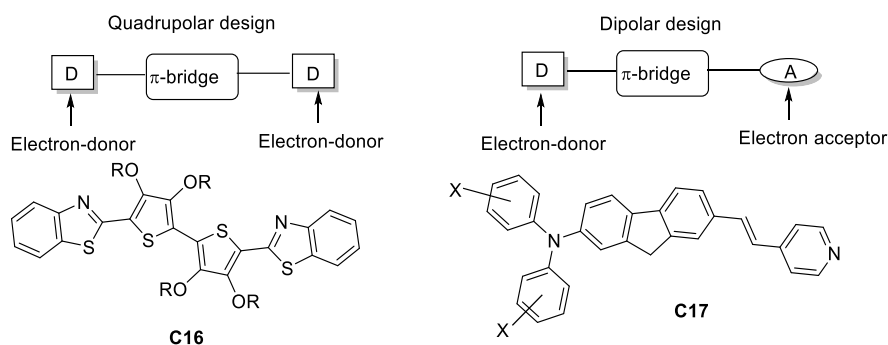


**Figure 22.** Examples of the most widely used molecular architectures TPA during the late 90s.

In 1996 Yuan et al. [47], reported the synthesis of a series of symmetric bis(dimesitylboryl) compounds and studied their second order hyperpolarizabilities ( $\gamma$ ) by third harmonic generation (THG) at 1.907  $\mu\text{m}$ .

Compound **B45** provided a larger  $\gamma$  value ( $229 \times 10^{-36}$  esu) than **C-18**, which has a very similar architecture (Figure 23). This is attributed to enhancement of the  $\pi$ -conjugation pathway due to the empty p-orbital on boron.

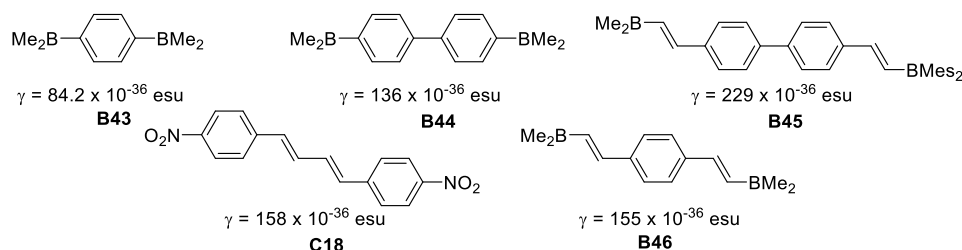


**Figure 23.** Second order hyperpolarizabilities for symmetric dimesitylboranes.

The enhancement of  $\gamma$  was achieved by increasing the length of the  $\pi$ -conjugation for both symmetric and unsymmetrical molecules. The MeS group was much more efficient than MeO for enhancing  $\gamma$ . Unsymmetrical “push-pull” organoboranes gave rise to large  $\gamma$  values (Figure 24).

The  $\gamma$  values in these boron compounds increase dramatically as the  $\pi$ -conjugation length increases. For unsymmetrical compounds, when comparing **B47**  $\gamma = 24 \times 10^{-36}$  esu, **B48**  $\gamma = 32 \times 10^{-36}$  esu, and **B49**  $\gamma = 23 \times 10^{-36}$  esu with **B60**  $\gamma = 93 \times 10^{-36}$  esu, **B58**  $\gamma = 81 \times 10^{-36}$  esu and **B59**  $\gamma = 54 \times 10^{-36}$  esu, the effect of the additional vinyl moiety is clearly greater for the strongest  $\pi$ -donor ( $\text{NMe}_2$ ) group.

By enhancing the charge transfer capabilities within the quadrupole architectures, Albota et al. [48] targeted TPA-efficient compounds by synthesizing molecules having the two different D- $\pi$ -A- $\pi$ -D and A- $\pi$ -D- $\pi$ -A topologies. Following this strategy, they reached  $\sigma$ TPA values in the range of 600–3700 GM (Figure 25).

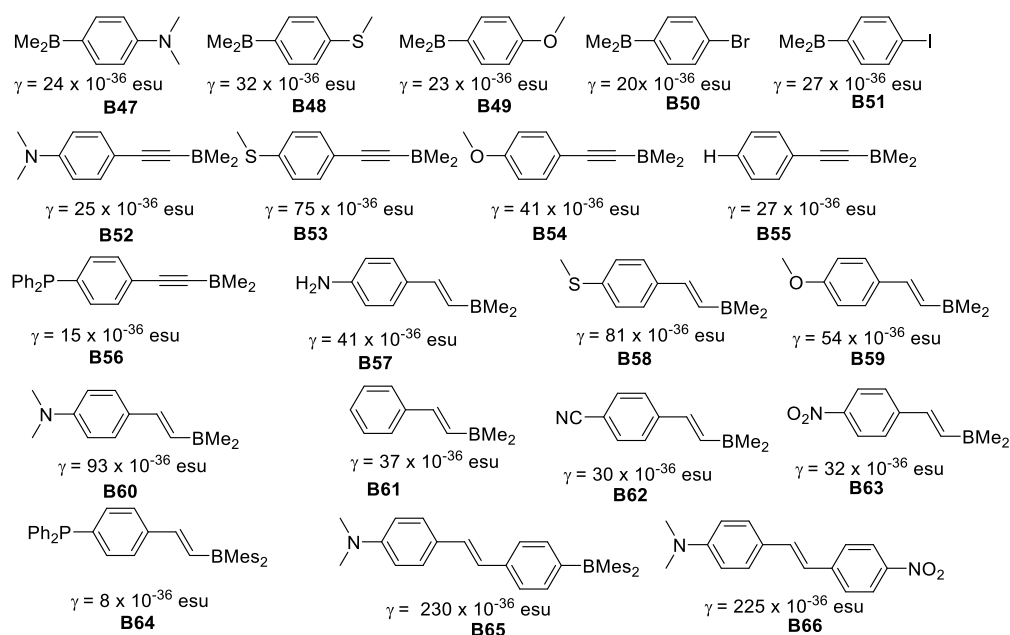


**Figure 24.** Second order hyperpolarizabilities for unsymmetric dimesitylboranes and  $\text{NO}_2$  analogous.

#### Quadrupolar design

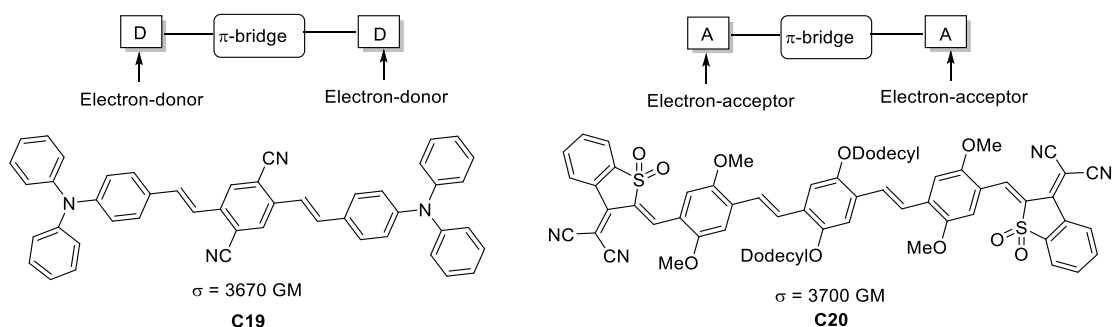


**Figure 25.** Most promising D- $\pi$ -A- $\pi$ -D and A- $\pi$ -D- $\pi$ -A molecular topologies in one-dimensional TPA chromophores.

Belfield et al. [49] synthesized “push-pull” molecules with different donating substituents, that exhibit  $\sigma_{\text{TPA}}$  of 650 and 1300 GM (Figure 26).

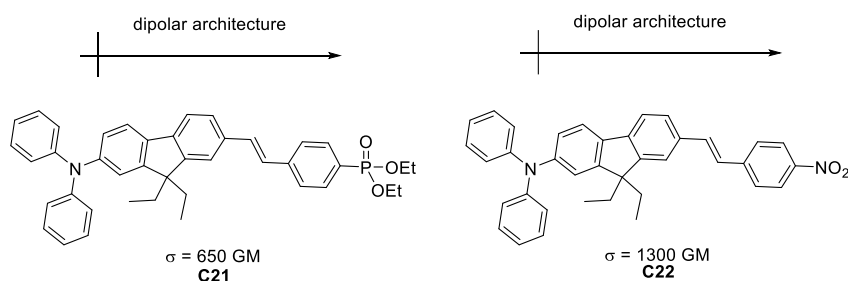


**Figure 26.** Efficient TPA chromophores designed within the dipolar approach.

At the beginning of the century, there was renewed interest in the electron-acceptor character of trivalent boron, with a special focus on the dimesitylboron group.

Several organoboron compounds were investigated with the aim of designing new materials with potential application in two-photon excited fluorescence (TPEF). Sensors and imaging are the

most targeted application for these materials, although applications in materials science were also envisioned during the early 2000s.

Chujo et al. [50], synthesized  $\pi$ -conjugated low molecular weight polymers, that exhibited strong photoluminescence. The compounds have a structure related to poly-*p*-phenylene vinylene with boron in the polymer chain and were prepared by hydroboration of aromatic and heteroaromatic diynes with mesitylborane. Compound **B67** based on diethynylbenzene displayed third-order nonlinear optical susceptibility  $\chi^{(3)} = 6.87 \times 10^{-6}$  esu, more than a thousand times larger than that of all-*trans*-polyacetylene, as measure by four-wave mixing (Figure 27).

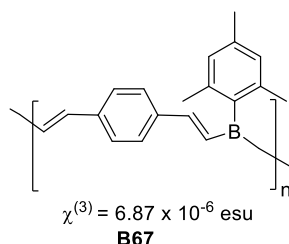


**Figure 27.** Polymer based on diethynylbenzene third-order nonlinear optical susceptibility value.

Liu et al. reported some of the most remarkable examples of these approaches both at the structural and synthetic level [51–53] between 2002 and 2004. These contributions illustrate the transition from the molecular architectures explored during the previous decade that worked to increase boron NLO second-order properties as well as from the general NLO design behind organic dipolar and quadrupolar topologies, all the way towards the fusion of both, to get to NLO, third-order, boron-including chemical structures with potential application due to their fluorescent properties.

Beginning with the dipolar structure, Liu examined different donors, and concluded that dimethylamino and diethylamino share, to a degree, the same donor character while carbazolyl and diphenylamino groups are above in the series. Two different  $\pi$ -bridges were explored to determine whether phenyl or thienyl are capable of delocalizing and connecting in a better way the two ends of the dipolar groups. Interestingly, when there is a dipolar architecture of this kind containing a phenyl, it was possible to reach up to 300 GM of  $\sigma_{TPA}$  for TPA (Figure 28).

When considering thiophene as an extension of the  $\pi$ -conjugation, Liu reported that the value of  $\sigma_{TPA}$  reached 239 GM, surpassing the properties of carbazole as a donor. This phenomenon proved the weak-donor character of thiophene along with its usual role as  $\pi$ -bridge. Another aspect is that changing the organoboron portion for a somewhat weak donor as benzothiazole to form a quadrupolar structure leads to a larger decrease in  $\sigma_{TPA}$  compared to a dipolar architecture.

Nowadays it is considered that multipolar structures will present better  $\sigma_{TPA}$ , provided they have an adequate design that allows interaction of the dipoles that leads to a good charge transfer.

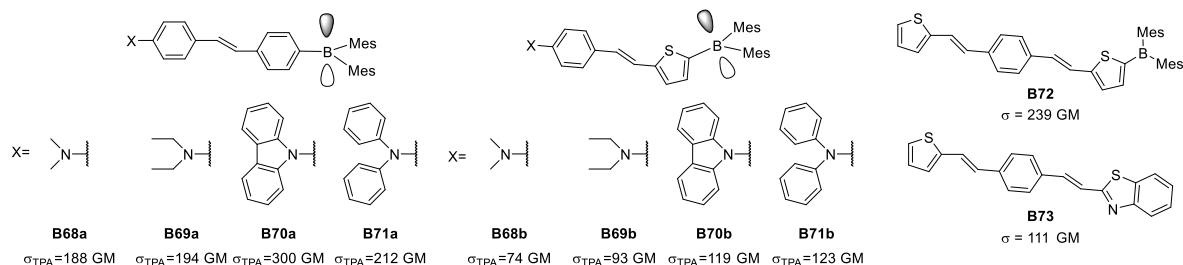


**Figure 28.** Some organoboron species studied during the early 2000s seeking enhanced TPA properties.

The quadrupolar structures depicted in Figure 29 were synthesized and their photophysical properties were measured to compare molecular architectures of the type Donor- $\pi$ -Donor with systems of the kind Acceptor- $\pi$ -Acceptor, containing trivalent boron species. Another factor studied was the

length of the  $\pi$ -system with one and two styryl units as  $\pi$ -bridge. This study demonstrated that  $\pi$ -conjugation is a key factor for attaining better TPA. In the particular case of the studied molecules, lengthening the  $\pi$ -bridge had a tenfold increase of the  $\sigma_{TPA}$ . This reasoning paved the way to build the molecule depicted in Figure 29 which presented an enhancement of 30 times its  $\sigma_{TPA}$ , compared to the species with one styryl unit as  $\pi$ -bridge.

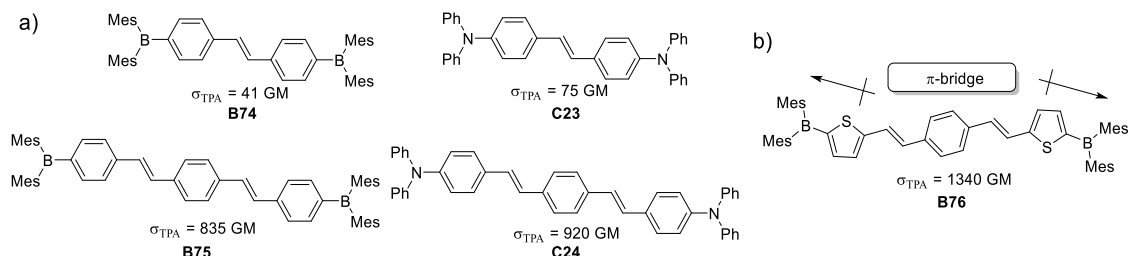


**Figure 29.** Quadrupolar organoboron species with different lengths of  $\pi$ -bridges. (a) Quadrupolar architectures varying the direction of electron density and  $\pi$ -bridge length; (b) design for TPA responsive molecule.

This architecture provides two somewhat strong dipoles at each end of the molecule (knowing that thiophene works as a weak donor), but the same thienyl portions have a second function to elongate the  $\pi$ -conjugation, combining in a remarkable manner both properties of that heterocycle.

Theoretical studies on this kind of systems (D- $\pi$ -D and A- $\pi$ -A motifs) by Tao et al. [54] provided information on the influence of changing the direction of electron density in quadrupolar architectures, as well as the effect of increasing the length of the  $\pi$ -conjugated system, establishing it as a function of the difference in dipole moments for the two-photon transition alongside charge redistribution within the donor or acceptor portions of the molecules. Having a large difference in dipole moment from the ground state to the excited state leads to a huge contrast in the atomic charges in the diphenylamino or diarylboron portions of the molecules.

In the early 2000s two contributions on the same kind of boron-based ligands but with two different applications were reported. On the one hand, Halik et al. [55] made use of the 1,3-dioxo ligand as acceptor unit to absorb two photons and through this photophysical process reduce and carry out the deposition of silver. The species used for this purpose, depicted in Figure 30, showed acceptable  $\sigma_{TPA}$  values, reaching up to 547 GM.

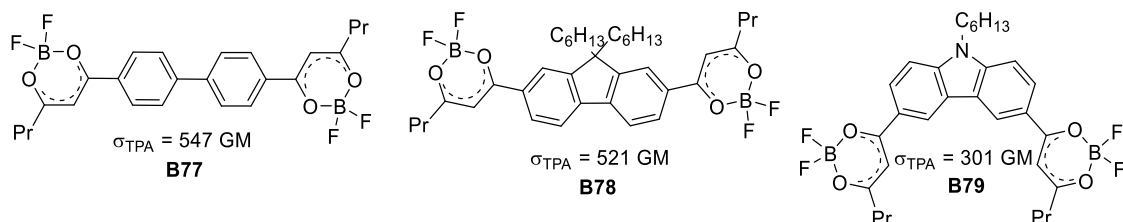


**Figure 30.** Series of compounds used for TPA-mediated photoreduction and deposition of silver.

The second series of molecules synthesized through this kind of ligands is that of Cogné-Laage et al. [56]. Mimicking the structural motif of boron dipyrromethene (BODIPY), a series of diaryl(methanato)boron complexes were synthesized and their TPA response was examined. According to the authors, the advantage of these complexes is the strength of the B–O bond which is less labile to hydrolysis than the B–N bond in BODIPYs.

The molecular architectures reported feature a quadrupolar design of the A- $\pi$ -A type. Even though tetravalent boron is considered an electron-donor moiety, its coordination modes entail a strong electron density deficiency on the ligands, especially when connected through a  $\pi$ -bridge to a

donor portion. This behavior distinguished organoboron from boron complexes from an electronic and structural standpoint. The molecular assortment proved having moderate NLO properties of 5–85 GM for  $\sigma_{TPA}$  values. Interestingly, one of the synthesized species reached 200 GM, this compound is depicted in Figure 31.

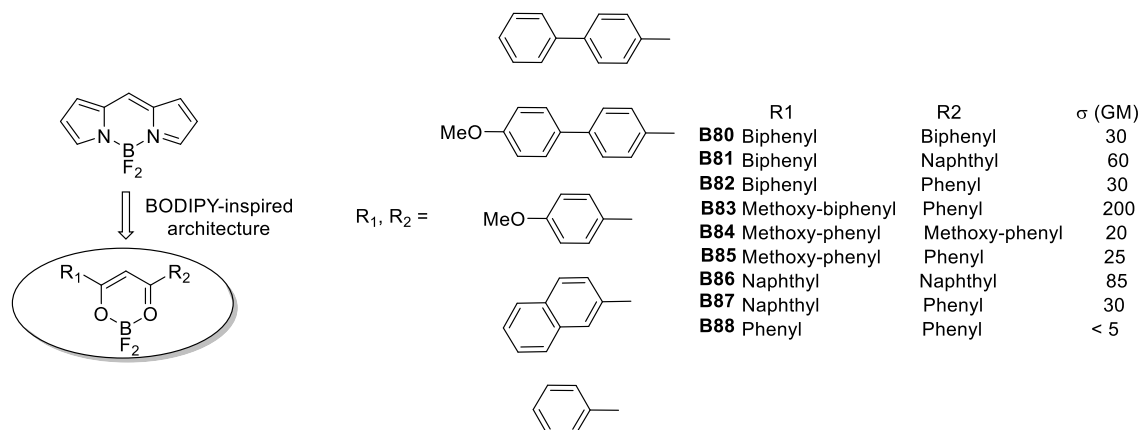


**Figure 31.** Diaroyl(methanato)boron complexes with aromatic portions as donors studied for their TPA responsiveness.

In 2006, Yuan et al., [57] synthesized and studied the nonlinear properties of a series of air-stable, conjugated dimesitylboranes (*p*-R-phenyl)dimesitylboranes substituted with various donor and acceptor groups: (*E*)-[2-(*p*-R-phenyl)ethenyl]dimesityl-boranes, (*E*)-[2-(2-thienyl)]dimesityl-borane and (*E*)-[2-(*o*-carboranyl)ethenyl]dimesitylborane. The first and second order molecular hyperpolarizabilities, determined by EFISH at 1.907  $\mu\text{m}$  in  $\text{CHCl}_3$  and THG measurements, revealed that compounds having strong R-substituent donors have the largest  $\beta$ . Hyperpolarizability values for these compounds were obtained from AM1 calculations with the exception of (*E*)-[2-(2-thienyl)]dimesityl-borane and (*E*)-[2-(*o*-carboranyl)ethenyl]dimesitylborane, and are in reasonable agreement with those determined experimentally, as well as with several hypothetical compounds containing multiple C=C bonds. The 2-(*p*-R-phenyl)ethenyl- and (*p*-R-phenylethynyl)dimesitylboranes showed larger  $\beta$  values than the analogous (*p*-R-phenyl)dimesitylboranes. The authors conclude that the increases in  $\beta$  for (*E*)-[2-(*p*-R-phenyl)ethenyl]dimesitylboranes compared to (*p*-R-phenylethynyl)dimesitylboranes may be due to larger changes in dipole moment in going from the ground to the excited state for the ethenyl derivatives.

THG measurements of  $\gamma_{\text{exp}}$  at 1.907  $\mu\text{m}$  showed again that (*E*)-[2-(*p*-R-phenyl)ethenyl]-dimesitylboranes and (*p*-R-phenylethynyl)dimesitylboranes have much larger  $\gamma_{\text{exp}}$  values than the analogous (*p*-R-phenyl)dimesitylboranes, as shown in Figure 32.

During the second part of the 2000s, Hayek et al. [58,59] and Nicoud et al. [60] introduced a new mode of delocalization of the type  $\pi$ - $\sigma$ - $\pi$  by using two boron and nitrogen containing heterocycles, alongside the now well established quadrupolar architecture. The systems used consisted of the 4-membered cyclodiborazane and the 6-membered pyrazabole. In both fragments, B–N sigma bonds are present and the cycles linked to the  $\pi$ -system, render the ring a delocalizing portion as well (as seen in Figure 33).

Analysis of the development of boron-based complexes to improve their photophysical properties, lead Hayek et al. to a pioneering, tandem theoretical-experimental approach where computational methods are used to explain atomistically the photophysical properties observed. By portraying the molecular orbitals involved in the main transitions that give origin to the absorption phenomenon, it is possible to visualize how the charge transfer increases in the NLO process for the 4-membered cyclodiborazane, in accordance with the  $\sigma_{TPA}$  value of 1350 GM shown by **B108**.

It is important to mention that the pyrazabole family of compounds has been used in bioimaging of HeLa cells using a concentration of  $10^{-6}$  M in DMSO, showing clear fluorescent staining of vesicles in the cytoplasm using laser power values up to 15 mW.

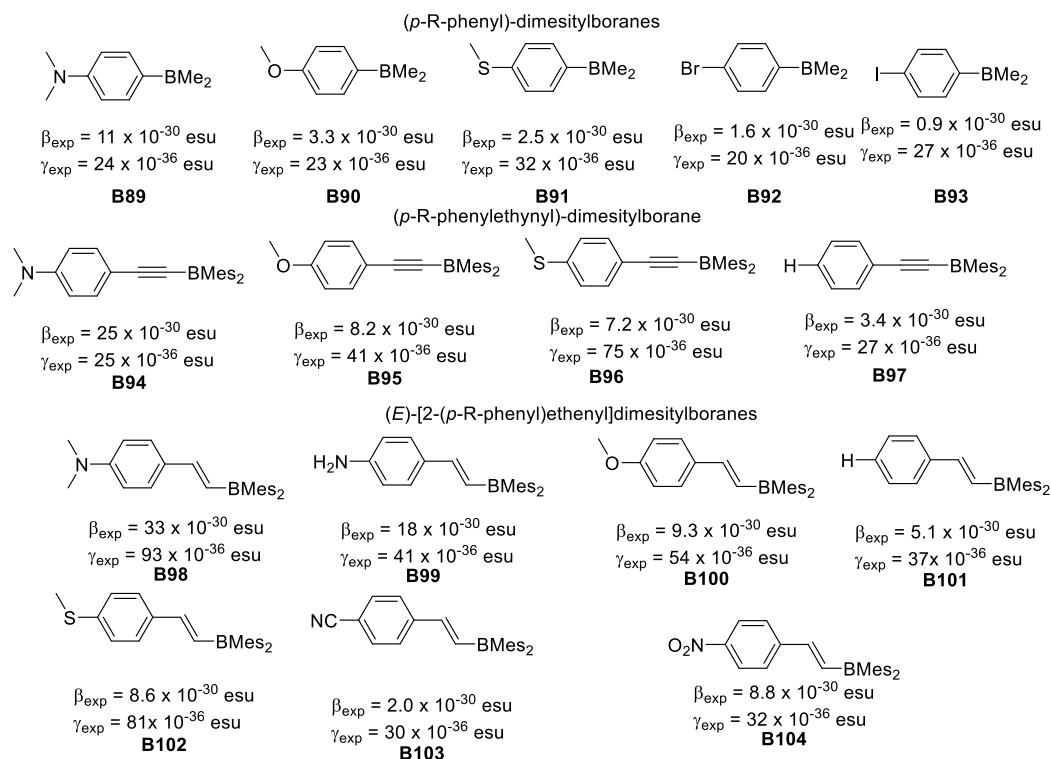


**Figure 32.** First and second order hyperpolarizabilities of conjugated dimesitylboranes.

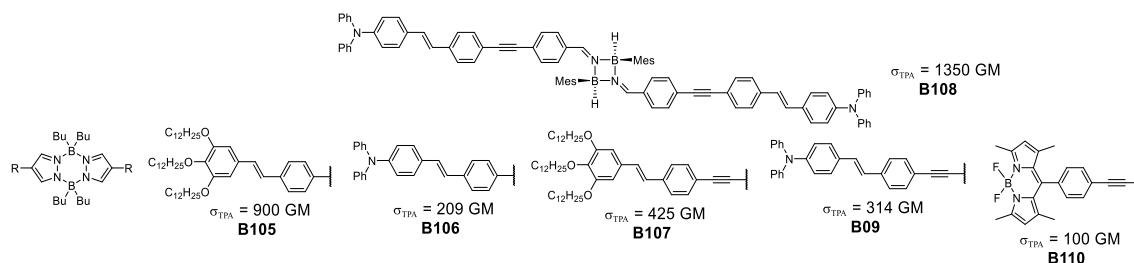


**Figure 33.** Cyclodiborazane and pyrazabole species developed for their TPA responsiveness.

A study by Ramos-Ortiz et al. of the NLO response [61] of a boron-imine complex formed by condensation between aminophenol and dimethylamino cinnamaldehyde (Figure 34), along with a crystal structure analysis of the packing and supramolecular interactions gave a moderate  $\sigma_{\text{TPA}}$  value similar to other reported molecules, which are more structurally complex.

In the last years, the development of TPA responsive boron-based compounds became multidisciplinary, increasing the knowledge of photophysical properties of the synthesized compounds as well as their applications.

It should be pointed out that TPA literature on BODIPY species is not included in the present work since this family of compounds has been extensively studied through the last 20 years.

To focus on the contributions of these last years to the field of TPA-responsive boron-based complexes, we have selected only some advancements of organoboron species in the field of NLO. These compounds have recently been reviewed by Ji and co-workers [38] providing an excellent overview of the knowledge within the field of trivalent organoboron species in the last 20 years and covering in detail the different applications of this chemical family, including an NLO section.

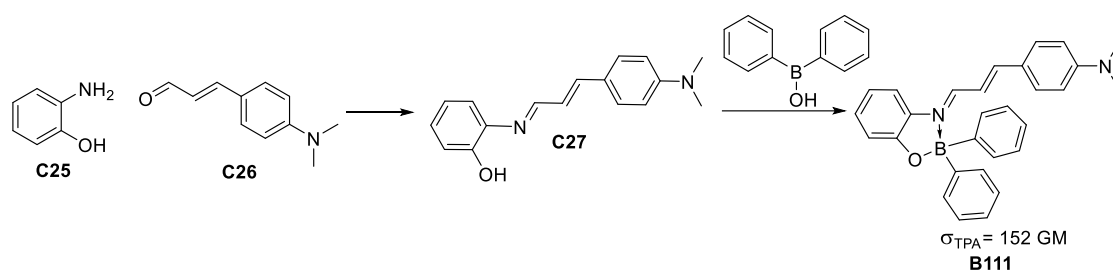


**Figure 34.** Scheme for obtaining a TPA-responsive boronate of major structural accessibility and  $\sigma_{TPA}$  value.

At the beginning of the decade, the tetravalent quadrupolar architectures were studied again by Li and co-workers [62] who synthesize a ligand based on a diazo dye. Reduction of the diazo group gave rise to a compound with tautomeric equilibrium, which is favored by the H-bonding present between the pyridine and the di-aza portion of the molecule. Coordination with  $\text{BF}_2$  to form the boron complex, leads to the compounds depicted in Figure 35. Although having a moderate  $\sigma_{TPA}$  value of 100 GM, computational calculations revealed that charge transfer was suppressed by coordinating with  $\text{BF}_2$  due to the fact that the HOMO–LUMO transition for the ligand shows better charge transfer from the pyridine portion to the H-bonded complementary subsystem. This is the main reason why the TPA measurements provide only a modest value for the photophysical property.

Jadhav et al. reinvestigated the pyrazabole core coupling this heterocycle to a series of  $\pi$ -spacers with ferrocene at the end to produce a number of molecules with the D- $\pi$ -A- $\pi$ -D architecture [63].

From the no- $\pi$ -spacer species to a set of phenylene derivatives, the photophysical and electrochemical properties were assessed to evidence the potential applicability of the synthesized compounds (as depicted in Figure 36). The results showed that the compounds with ethynyl-phenyl and the one with diethynyl-phenylene as substituents connecting the pyrazabole and ferrocene portions, presented the best  $\sigma_{TPA}$  values when testing their TPA responsiveness, providing values of 831 and 1016 GM, respectively. This is in accordance with the delocalization pattern present in the molecules. As the  $\pi$ -conjugation increases, the TPA response increases too. In addition, changing the direction of the delocalization affects importantly the magnitude of the  $\sigma_{TPA}$ .

Finally, it is important to address the contribution of D'Aléo's group revisiting the hydroxyketone functionality coordinated to a  $\text{BF}_2$  moiety exploited during the early 2000s by Halik [55], Cogné-Laage [56], D'Aléo [64], Lanoë [65] and Kamada [66] in three separate studies.

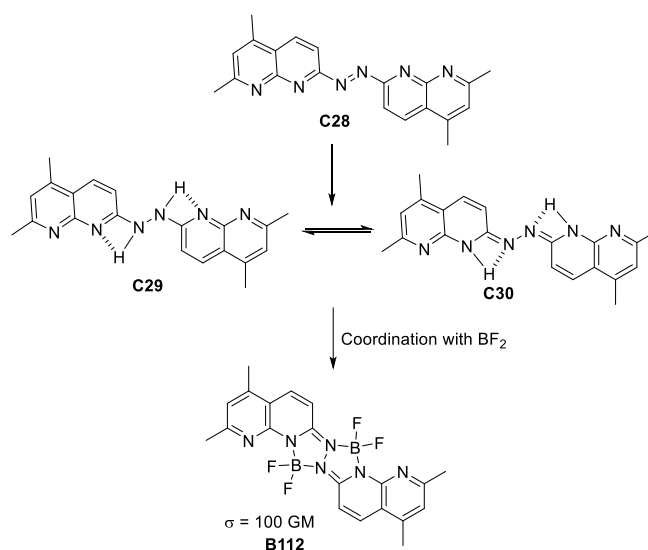


**Figure 35.**  $\text{BF}_2$ -based, hydrazine-coordinated species of quadrupolar architecture presenting TPA.

Using curcuminoid derivatives, D'Aleo was able to tune these substituents into pseudoquadrupolar architectures and actual quadrupoles that exhibited a TPA response. Besides having these two electron-donating-substitution differences, the direction of electron density is changed by varying the angle of the two dipoles assembled within the molecules.

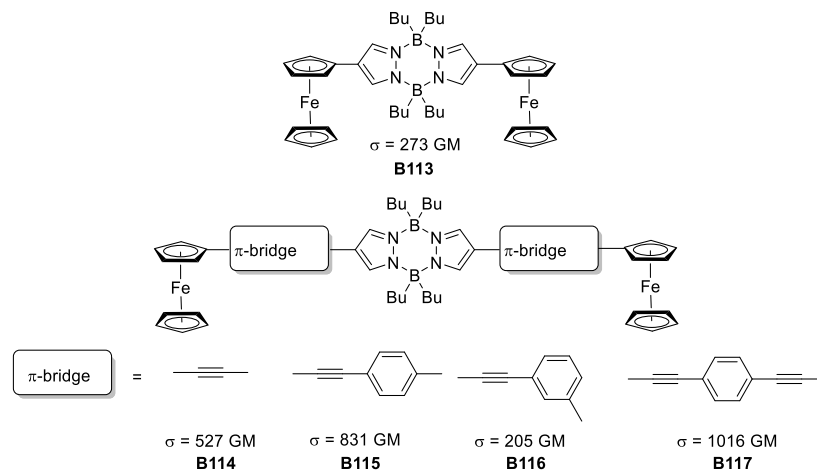


Figure 36. Quadrupolar molecules based on pyrazabole  $\pi$ -bridged with ferrocene.

The molecules in Figure 37 evidence the effect of different electron-donating groups and how rigidity of the conjugation is the key to reach high  $\sigma_{TPA}$  values. The best results are obtained with nitrogen donors while the efficiency is reduced when using sulfur and finally oxygen. Additionally, a change in symmetry from quadrupolar to dipolar importantly reduces the TPA response.

Another way to affect the TPA response is to change the angle at the quadrupole. The three V-shaped quadrupolar boron complexes depicted in Figure 38, show decreased values of  $\sigma_{TPA}$ . This is important evidence to consider because when TPA response is the goal, then the quadrupolar and linear molecular architecture with good rigid donors should be chosen. Additionally, having V-shaped compounds with moderate  $\sigma_{TPA}$  values opened the possibility for different applications, for example, greater viability to obtain crystalline solids, which show fluorescent properties. This could lead to new developments in boron-based emitting solids.

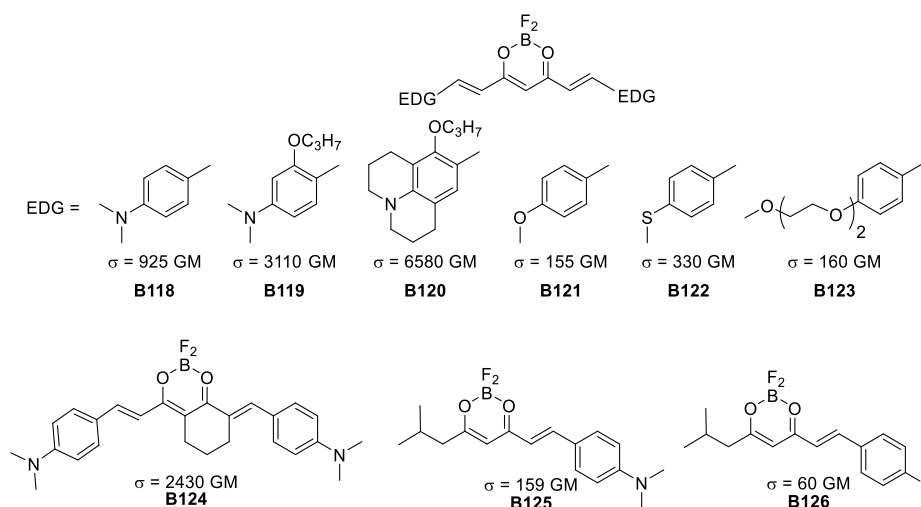


Figure 37. Quadrupolar  $\text{BF}_2$ -coordinated hydroxyketones.

These two studies approach the problem of how the electron density distributes, through quantum-level computations and allows to visualize the way charge transfer proceeds via

HOMO–LUMO from the ligands to the tetravalent boron moiety of the molecules. They also highlight the importance of an atomistic and electronic point of view that provides a connection between the design, the synthesis, the way the molecules interact electronically and the applications they present.

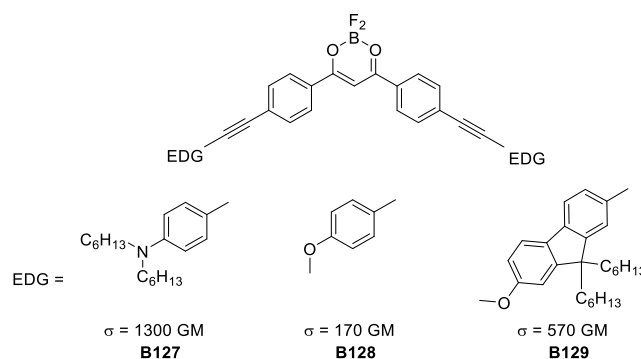


Figure 38. V-shaped boron-based,  $\text{BF}_2$ -coordinated hydroxyketone complexes with TPA response.

### 3. NLO properties in Organotin Compounds and Tin Complexes

#### 3.1. Second-Order NLO Properties

In 1991, Mingos et al. [67] reported the first examples of SHG in organotin compounds for 16 organotin(IV) derivatives with trisubstituted catecholato ligands (Figure 39), for which the SHG intensity in solid state was measured at 1.064 and 1.907  $\mu\text{m}$  compared to urea (Table 2).

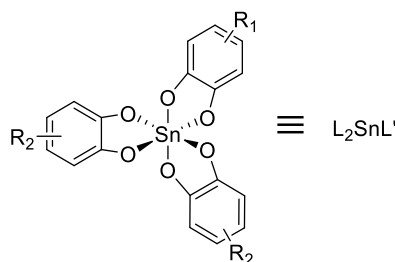


Figure 39. Structure of the catechol tin compounds.

These materials can be classified in three groups: The first group shows larger SHG efficiency at 1.064  $\mu\text{m}$  than at 1.907  $\mu\text{m}$  (**Sn2** and **Sn5**) and it corresponds to a resonance effect when the double frequency gets close to the energy of the charge transfer transition; the second group shows larger SHG efficiency at 1.907  $\mu\text{m}$  than at 1.064  $\mu\text{m}$  (**Sn6** and **Sn11**), this is due to residual absorption observed at 532 nm reducing the efficiency at 1064 nm; the third group in which the efficiencies observed at 1.064 and 1.907  $\mu\text{m}$  (**Sn3**) are the same.

Although it is difficult to fully rationalize the data gathered in Table 2, there is a trend for enhanced efficiency when electron-acceptor groups are present. This is consistent with an overall donating capability associated to the “ $\text{SnO}_6$ ” core.

Table 2. Measured second-harmonic signals at 1.064 and 1.907  $\mu\text{m}$  wavelengths relative to urea.

#	R <sub>2</sub>	R <sub>1</sub>	1.064 $\mu\text{m}$	1.907 $\mu\text{m}$	#	R <sub>2</sub>	R <sub>1</sub>	1.064 $\mu\text{m}$	1.907 $\mu\text{m}$
<b>Sn1</b>	H	H	0.4	0	<b>Sn9</b>	3-MeO	3-MeO	0.01	0.03
<b>Sn2</b>	H	4-NO <sub>2</sub>	0.28	0.17	<b>Sn10</b>	3-MeO	H	0.08	0
<b>Sn3</b>	H	3-MeO	0.19	0.12	<b>Sn11</b>	3-MeO	4-NO <sub>2</sub>	0.14	0.32
<b>Sn4</b>	H	3,4,5,6,4-Cl	0.07	0.05	<b>Sn12</b>	3-MeO	3,4,5,6,4-Cl	0	0
<b>Sn5</b>	4-NO <sub>2</sub>	4-NO <sub>2</sub>	1.33	0.44	<b>Sn13</b>	3,4,5,6-4Cl	3,4,5,6,4-Cl	0	0
<b>Sn6</b>	4-NO <sub>2</sub>	H	0.14	0.71	<b>Sn14</b>	3,4,5,6-4Cl	H	0	0
<b>Sn7</b>	4-NO <sub>2</sub>	3-MeO	0	0	<b>Sn15</b>	3,4,5,6-4Cl	4-NO <sub>2</sub>	0	0
<b>Sn8</b>	4-NO <sub>2</sub>	3,4,5,6,4-Cl	0	0	<b>Sn16</b>	3,4,5,6-4Cl	3-MeO	0	0

In 1994, Lequan et al. [68,69] studied the effect of the length of the electronic conjugation pathway on the first hyperpolarizability ( $\beta$ ) for four organotin compounds with octupolar geometry. Owing to the apolar character of the octupolar species, the EFISH technique commonly used for  $\beta$  measurements, had to be replaced by the alternative HRS (Hyper-Rayleigh Scattering). As shown in Table 3,  $\beta$  increases with an increase in the conjugation length.

**Table 3.** Nonlinear optical properties for the tetraorganotin derivatives.

#	Compound	$\beta_{xyz} \times 10^{-30}$ esu
<b>Sn17</b>	$\text{Sn}(\text{C}_6\text{H}_4\text{NMe}_2)_4$	13.0
<b>Sn18</b>	$\text{Sn}(\text{C}_6\text{H}_4\text{C}_6\text{H}_4\text{NMe}_2)_4$	24
<b>Sn19</b>	$\text{Sn}(\text{C}_6\text{H}_4\text{N}=\text{NC}_6\text{H}_4\text{NMe}_2)_4$	159
<b>Sn20</b>	$(\text{C}_6\text{H}_5)\text{Sn}(\text{C}_6\text{H}_4\text{N}=\text{NC}_6\text{H}_4\text{NMe}_2)_3$	$\beta_{zzz} = 181$

In 2000, Fiorini et al. [70] studied an analog of compound **Sn19**. Using an all-optical orientation experimental setup, Fiorini studied dynamics and symmetry in PMMA (Poly(methyl methacrylate)) rods; observing that under all-optical poling conditions, *cis/trans* isomerization of the azobenzene moieties proceeds to an efficient molecular reorientation that leads to a SHG response.

In 2004, Farfán and Lacroix et al. [71] published four diorganotin compounds with “push-pull” structures (Figure 40) for which  $\beta$  was measured and compared to its related diorganoborates [30].

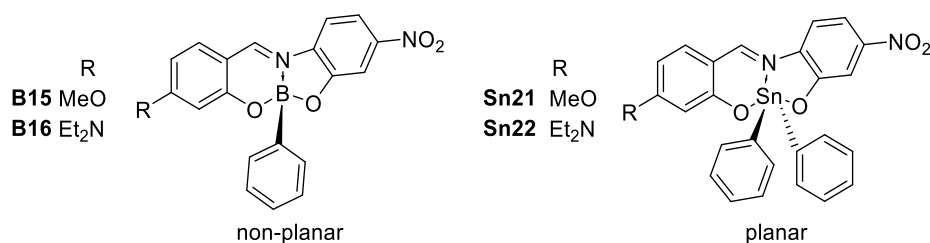


**Figure 40.** Diorganotin and corresponding diorganoboron as representative members of these families of complexes.

The X-ray diffraction study showed that the torsion angle between the methoxyphenyl and the nitrophenyl moieties is  $8.1^\circ$  in the diorganotin compound and  $11.4^\circ$  for the diethylamino and increases to  $31.2^\circ$  in the organoboron compound, additionally the structure reveals a planarity in the C–C=N–C connecting bridge, imposed by the diorganotin fragment. This increased planarity results in a better delocalization over the  $\pi$ -conjugated structure and an increase in the  $\beta$  value equal to 80% and 36% for the methoxy and dimethylamino derivatives (Table 4), respectively.

During 2006, two main contributions on NLO properties of diorganotin compounds were highlighted. On the one hand, analysis of a series of organotin coordination compounds of complex structure with a polyoxotungstate ligand carried out by Guand and co-workers [72] highlighted the relevance of theoretical studies (Figure 41).

**Table 4.** Second-order NLO properties for the diorganotin and diorganoborate compounds.

#	R	$\beta \times 10^{-30}$ esu	$\mu$ (D)
<b>Sn21</b>	OCH <sub>3</sub>	48.9	10.2
<b>B15</b>	OCH <sub>3</sub>	27.0	10.2
<b>Sn22</b>	NEt <sub>2</sub>	-	-
<b>B16</b>	NEt <sub>2</sub>	-	-

Through quantum calculations, Guan was able to determine that the charge transfer along a preferred axis of the molecules is of chief importance for NLO response. This study points out three main factors in which NLO properties are tuned: (1) Size of a heavy heteroatom in the structure (Ge

gives the best); (2) lengthening of the conjugation in the organotin portion; and (3) the presence of an electron-acceptor at the end of this same moiety to enhance the charge transfer capabilities, as determined by calculating dipole polarizabilities and analyzing the frontier orbital contour plots for the complexes.

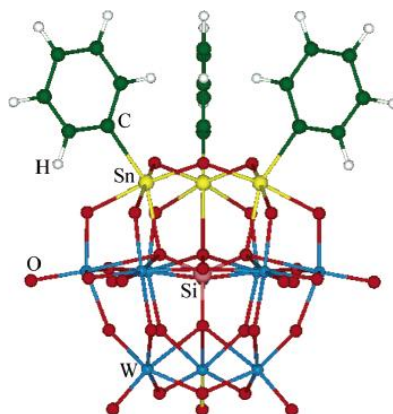


**Figure 41.** Theoretical studies of polyoxotungstate- $R_3Sn$  for the prediction of second-order NLO response. (Reprinted with permission from [72], Guan, W.; Yang, G.; Yan, L.; Su, Z. Prediction of second-order optical nonlinearity of trisorganotin- substituted  $\beta$ -Keggin polyoxotungstate. Copyright 2006 American Chemical Society.)

That same year, Farfán and Lacroix reported a series of tin-based complexes coordinated to chiral aminoalcohols [73] and chiral aminoacids [74] through the synthesis of Schiff bases (Figure 42). These synthetically accessible coordination compounds were studied through different aspects. First of all, the crystal structures proved the viability to obtain these complexes as non-centrosymmetric solids, which is a main factor to consider for second-order NLO applications in the solid state.

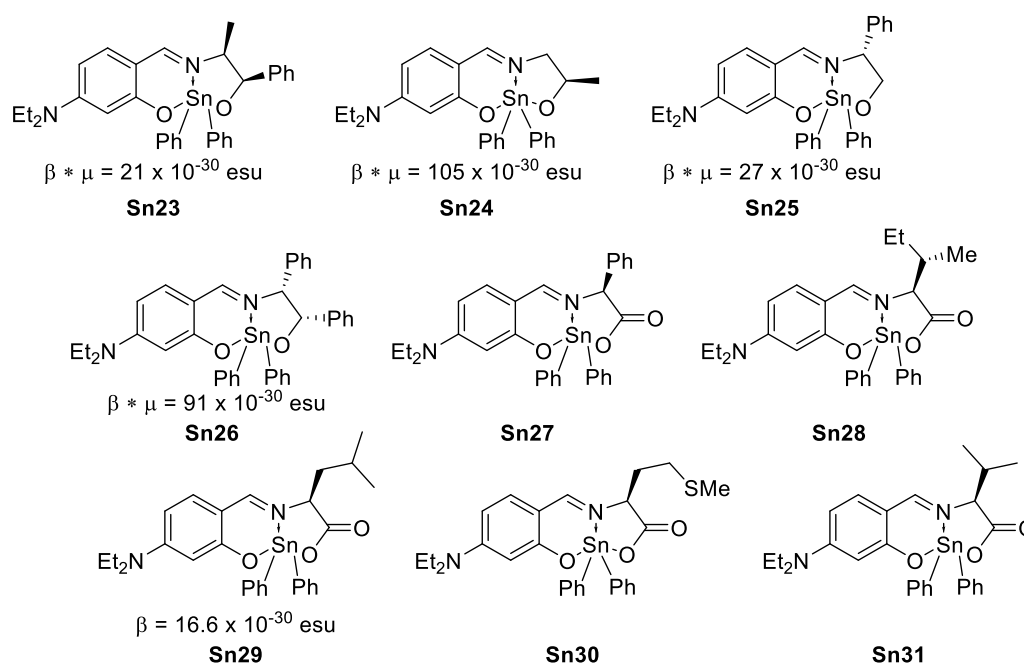


**Figure 42.** Aminoalcohols and aminoacids derived Schiff-base-Tin complexes.

The introduction of a chiral moiety is the only strategy that guarantees a non-centrosymmetric space group in the solid state, which is one of the parameter required for  $\chi^{(2)}$  (quadratic susceptibility in Equation (2)). This study provided a unique example of a series of molecules with the same NLO

response arising from the  $\text{Et}_2\text{N}$  to  $\text{C}=\text{N}$  charge transfer unit present in all cases, that crystallize in the same chiral space group, and has the same asymmetric unit cell content. The results allowed to propose a correlation between the solid state SHG response and a molecular geometrical parameter defined as the “degree of chirality”  $d\chi$ , in Figure 43.

At the end of the decade, Kumar and co-workers [75] obtained a pseudocage, oxygen-bridged organotin complex (Figure 44) and performed a thorough structural analysis of the crystalline solid obtained. A computational approach on this complex indicated a clear HOMO–LUMO-based charge transfer transition from the periphery of the ligands to the pseudocage formed by the tin and oxygen atoms. As a final part of this study, computational calculations of four analogues and prediction of their second-order NLO properties, revealed that changing the ligands to a multipolar architecture containing two strong electron donors would function as the best candidate to express NLO responsiveness.

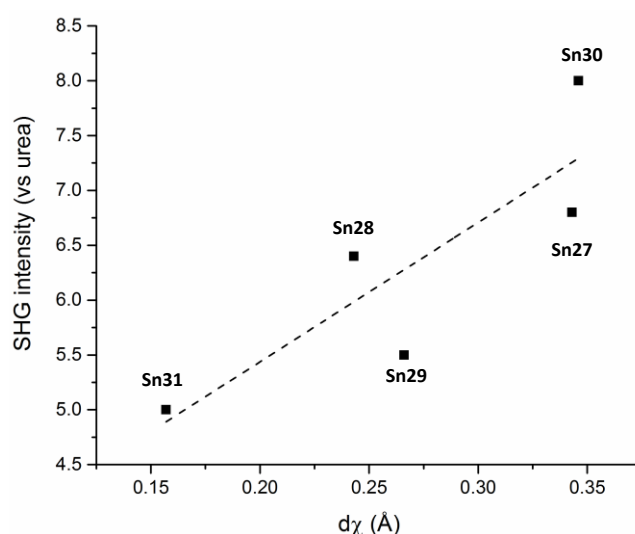


Figure 43. SHG intensities as a function of the degree of chirality ( $d\chi$ ).

In 2014, Farfán and Santillan et al. [76] reported six hexacoordinated organotin compounds (Figure 45) with NLO properties; Table 5 shows a trend for the  $\beta \times \mu$  product which decreases in the order:  $\text{Sn}(\text{Ph})_2$  (**Sn37**) >  $\text{Sn}(n\text{-Bu})_2$  (**Sn36**) >  $\text{Sn}(\text{Me})_2$  (**Sn35**).

In 2015, Şirikci et al. [77] performed a theoretical study on five organotin(IV) compounds (Figure 46) previously reported [78–81], in which they computed several constants (HOMO–LUMO, polarizabilities, geometric parameters,  $^1\text{H}$  and  $^{13}\text{C}$ -NMR chemical shifts, chemical reactivity descriptors) through DFT using seven different functionals. This investigation was carried out to examine which functional describes more adequately a certain parameter in this type of organotin complexes.

Table 5. Nonlinear optical properties for the hexacoordinated tin compounds.

$\text{R}_1$	$\beta$ (calc.) <sup>a</sup>	$\mu$ (calc.) <sup>a,b</sup>	$\beta \times \mu$ (calc.)	$\beta \times \mu$ (exp.)
<b>Sn33</b>	19.0	2.07	25.7	-
<b>Sn35</b>	-	1.23	-	14.8
<b>Sn36</b>	19.0	1.35	12.0	48.2
<b>Sn37</b>	19.9	1.64	13.2	56.4

<sup>a</sup> from DFT calculations in  $10^{-30}$  esu; <sup>b</sup> in D.

In their work, Şirikci determined the theoretical static second-order hyperpolarizability ( $\beta$ ) in chloroform observing the same trend whatever the functional used, **Sn41** < **Sn38** < **Sn40** < **Sn42** < **Sn39** and obtained values in the range of  $4.25\text{--}13.40 \times 10^{-30}$  esu. However, when the non-hybrid

functionals HTCH and TPSSTPSS were used the trend was reversed for **Sn39** and **Sn42**, as shown in Figure 47.

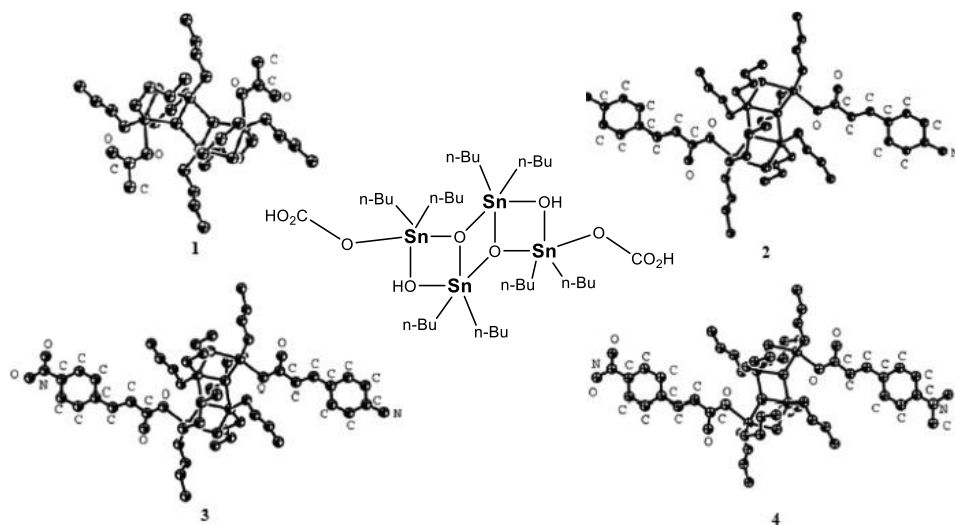


**Figure 44.** Computationally calculated species for pseudocage, oxo-bridged tin complexes with potential second-order NLO response. (Reprinted from [75], Kumar, A.; Prasad, R.; Kociok-Köhn, G.; Molloy, K.C.; Singh, N. Synthesis, structure and calculated NLO properties of  $[(n\text{-Bu})_2\text{Sn}-\mu\text{-O}-\mu\text{-OH}-\text{Sn}(n\text{-Bu})_2(\text{CH}_3\text{CO}_2)]_2$  and its putative derivatives. Copyright 2009, with permission from Elsevier.)

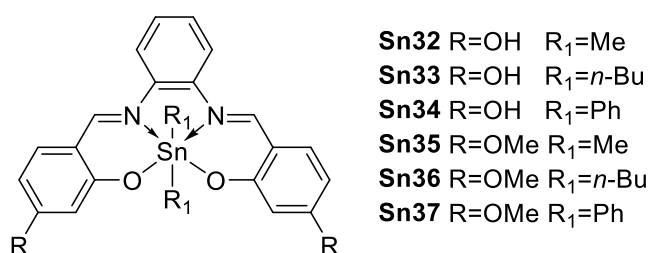


**Figure 45.** Hexacoordinated tin compounds.

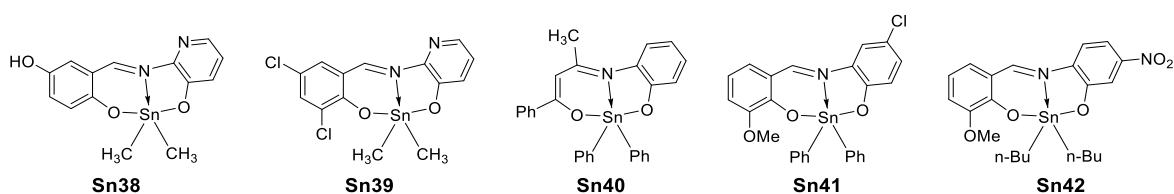


**Figure 46.** Organotin compounds investigated by Şirikci et al. [77].

A series of chalcogenides was reported by Dehnen et al. [82,83] in 2016, where the organic ligand was interchanged by methyl (**Sn43**), 1-naphthyl (**Sn44**), *p*-styryl (**Sn45**) and phenyl (**Sn45a**) (Figure 48); to understand the role of the substituents in SHG.

In the solid state, a strong SHG signal was observed for the chalcogenides containing the methyl and 1-naphthyl substituents, while a strong white-light emission was observed for the *p*-styryl and phenyl substituents. From this, it was inferred that **Sn43** and **Sn44** must be highly ordered in the solid state as compared to **Sn45** and **Sn45a** (due to the intrinsic requirements for SHG). Indeed, the small methyl group and its lack of flexibility could increase the ordering in the solid state for compound **Sn43**; for compound **Sn44** the naphthyl ligand produces  $\pi$ - $\pi$  stacking which apparently induces high ordering too.

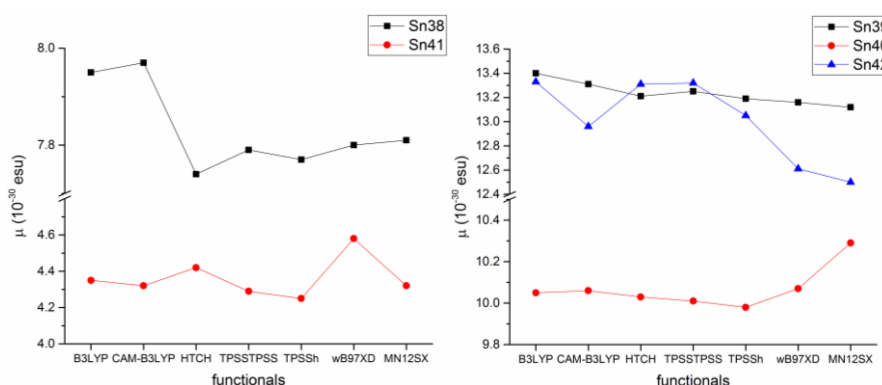


Figure 47.  $\beta$  obtained for the organotin compounds with different functionals.

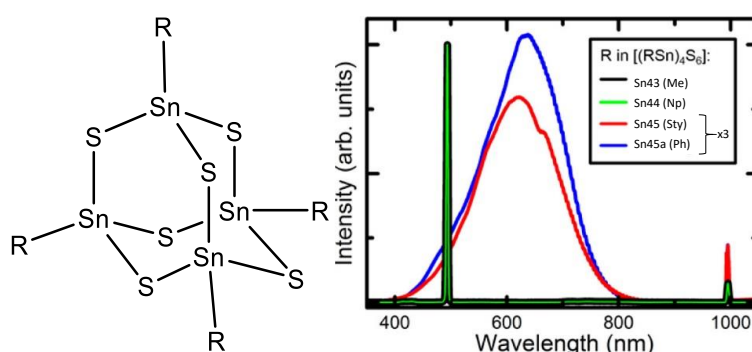


Figure 48. Chalcogenides reported by Dehnen et al. (Adapted with permission from [82], Rosemann, N.W.; Eußner, J.P.; Dornsiepen, E.; Chatterjee, S.; Dehnen, S. Organotin Chalcogenide Clusters: Between Strong Second-Harmonic and White-Light Continuum Generation. Copyright 2016 American Chemical Society.)

For the chalcogenide with naphthyl as ligand, supramolecular stacking is favored, this order yields a crystalline phase which is non-centrosymmetric and SHG responsive. In the case of phenyl and styryl as substituents, the order decreases because dispersive interactions surpass  $\pi$ - $\pi$  stacking. Losing the non-centrosymmetric arrangement but keeping the electron delocalization in the long  $\pi$ -system makes more plausible the *bremsstrahlung* effect [84,85] producing the white supercontinuum observed in the emission spectra, which corresponds not only to the remains of the second-order effect but also to the appearance of other nonlinear contributions due to the *bremsstrahlung*.

In 2016, Dang et al. [86] reported the  $\text{NH}(\text{CH}_3)_3\text{SnX}_3$  ( $\text{X} = \text{Cl}, \text{Br}$ ) orthorhombic hybrid perovskite single crystal. The distorted pyramidal structure of tin ( $\text{SnX}_3$ ) generated asymmetry in the  $\text{NH}(\text{CH}_3)_3\text{SnX}_3$  unit. The acentric crystal allowed to study its powder SHG for both compounds, which at 1064 nm shows a signal 1–2.5 times vs. KDP; further measurements proved that the SHG intensity depends on the particle size, when its size increases the SHG signal decreases, showing that they are not type-1 phase matchable materials [87]. With an increase of temperature, the SHG intensity decreases during the phase transition. The change of SHG was reversible showing overlapping curves in the cooling and heating runs.

### 3.2. Third-Order NLO Properties

In 1999, Sing et al. [88] reported for the first time five tin(IV) porphyrins complexes with different axial ligands attached to the metallic center having third order NLO properties at 802 nm. In these compounds, the measured values of  $\gamma$  were negative indicating a self-defocusing character; and  $\gamma$  increases as the electron donating capacity of the axial ligand decreases (Figure 49).

The enhanced  $\gamma$  value for **Sn50** ( $X = I^-$ ) is a result of the strong interaction between the soft acid Sn(IV) in the porphyrin and the soft base  $I^-$ . This interaction increases the electron density in the porphyrin core which normally enhances the hyperpolarizability as confirmed by the UV-Vis Q band of the porphyrins that shows a bathochromic shift following the same trend as  $\gamma$ .

Rao and Kiram et al. [89,90] reported the non-linear absorption (NLA) properties for five oligomers of tin(IV) porphyrins (two are shown in Figure 50) and their correlation with TPA and excited state absorption (ESA). The results for these systems indicate that the ratio of the excited and ground state cross sections ( $\sigma_{\text{Ex}}/\sigma_g$ , Table 6) are large enough to promote ESA.

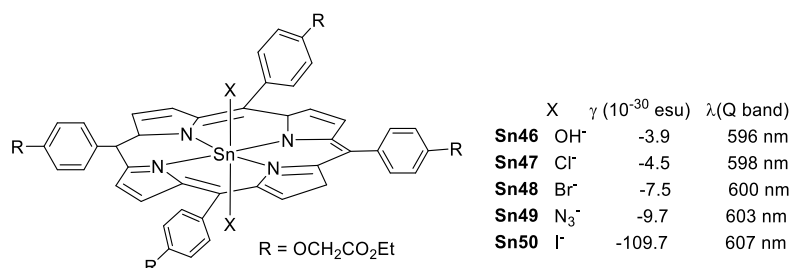


Figure 49. Structure of tin(IV) porphyrins with different axial ligands,  $\gamma$  and  $\lambda_{\text{max}}$  (nm) values.

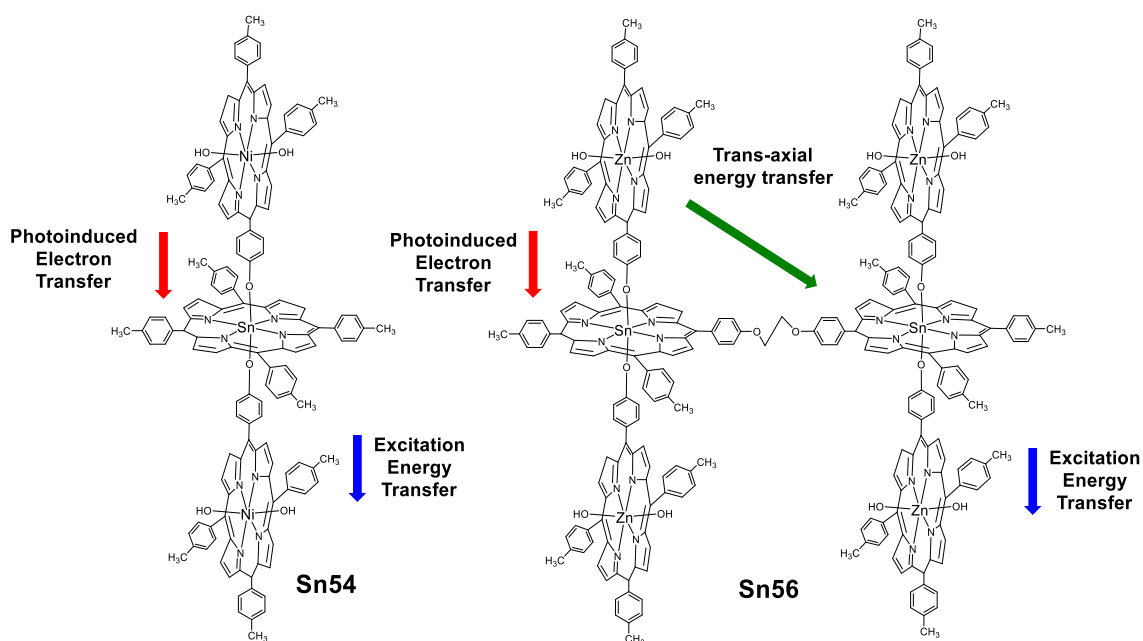


Figure 50.  $\text{Sn-Ni}_2(\text{TTP})_3$  and  $\text{Sn}_2\text{-Zn}_4(\text{TTP})_6$  oligomers of porphyrins.

The lifetimes of the highest excited singlet state ( $\tau_s$ ) for these oligomers of porphyrins are far more rapid than intersystem crossing ( $\tau_{\text{ISC}}$ ), as expected, however because the lifetime of  $S_1$  is close to the laser pulse width and the fluorescence quantum yield is low, some of the molecules seem to transfer to  $T_1$ . The  $\sigma_{\text{TPA}}$  obtained are in the range of  $2.7\text{--}396 \times 10^{-4}$  GM, the largest one is  $396 \times 10^{-4}$  GM for the trimer **Sn54** which is 146 times larger than the monomer **Sn51**. This can be rationalized as a result of photoinduced electron transfer (PET), excitation energy transfer (EET) and trans-axial energy transfer processes which occur simultaneously in these oligomers, leading to a higher delocalized singlet excited state enhancing the TPA assisted by ESA (which is also improved by the resonance of the excitation wavelength with the Q band).

As in porphyrins, tin phthalocyanines (Figure 51) also shows NLA with a good ratio  $\sigma_{\text{Ex}}/\sigma_g$  making them able to promote ESA and enhance reverse saturation (RSA) which is suitable for optical limiting (OL).

**Table 6.** Optical properties of the oligomers described by Rao and Kiram et al. [89,90].

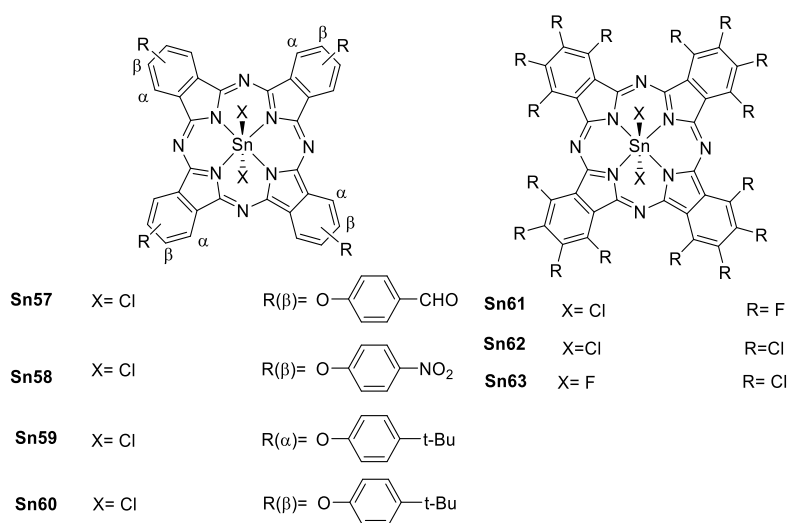
#	Porphyrin	$\gamma^a$	$\beta^b$	$\sigma_{TPA}^c$	$\sigma_{Ex}/\sigma_g$	$\tau_S^d$	$\tau_{ISC}^d$	$\tau_{FI}(\Phi\%)^e$
<b>Sn51</b>	Sn(TTP)	0.37	0.45	2.7	3.24	60	1000	0.56 (71), 1 (28)
<b>Sn52</b>	Sn-Sn(TTP) <sub>2</sub>	3000	1.50	13.6	21.53	7.5	180	0.57 (95), 4.94 (5)
<b>Sn53</b>	Sn-(H <sub>2</sub> ) <sub>2</sub> (TTP) <sub>3</sub>	930	-	-	7.26	500	380	0.74 (71), 5.93 (28)
<b>Sn54</b>	Sn-Ni <sub>2</sub> (TTP) <sub>3</sub>	610	1.45	396	6.21	50	550	0.62 (70), 2.13 (29)
<b>Sn55</b>	Sn <sub>2</sub> -(H <sub>2</sub> ) <sub>4</sub> (TTP) <sub>6</sub>	330	-	-	19.45	500	220	0.45 (28), 1.95 (23), 7.25 (47)
<b>Sn56</b>	Sn <sub>2</sub> -Zn <sub>4</sub> (TTP) <sub>6</sub>	380	0.90	15.7	6.73	15	600	0.66 (30), 1.73 (69)

<sup>a</sup>  $\gamma$  in  $10^{-30}$  esu, <sup>b</sup>  $\beta$  in  $10^{-9}$  cm $\cdot$ W $^{-1}$ , <sup>c</sup>  $\sigma_{TPA}$  in  $10^4$  GM, <sup>d</sup>  $\tau_S$  and  $\tau_{ISC}$  in ps, <sup>e</sup>  $\tau_{FI}$  in ns; obtained in CHCl<sub>3</sub>.

Wöhrle et al. [91,92] reported a series of tin(IV) and Ge(IV) phthalocyanines that were studied both in solution and in thin films of polymers to enhance their OL properties (Figure 51). Comparing the free base with its respective germanium(IV) and tin(IV) phthalocyanine,  $\beta$  is larger when a metallic center is present, and it is even larger for the tin complexes. These results correlate with the size of the metallic center (heavy atom effect).

Comparison of the electronic effect of the substituents in different positions [93] of the phthalocyanine shows, that there is a considerable increase in  $\beta$ ,  $\sigma_{TPA}$  and  $\text{Im}\{\chi^{(3)}\}$  ( $\text{Im}\{\chi^{(3)}\}$  is the imaginary part of the third order hyperpolarizability) for the  $\alpha$  position compared to  $\beta$  position (Table 7). This is attributed to a less polarizable electronic structure for the  $\beta$  isomer, also it is known that the substituents located at the  $\alpha$  position have more influence in the electronic distribution of the phthalocyanine than those in the  $\beta$  position [94].

When comparing the different substituents there is not a considerable change in  $\beta$  in the case of the aldehyde or the nitro group, but for the *t*-butyl  $\beta$  is larger. This is explained by the increase of the polarization towards the metallic center in terms of a better electron-donating group (Table 7).

**Figure 51.**  $\alpha$ - and  $\beta$ -substituted tin(IV) phthalocyanines.**Table 7.**  $\beta$ ,  $\text{Im}\{\chi^{(3)}\}$  and the ratio  $\sigma_{Ex}/\sigma_g$  for some phthalocyanines.

#	$\beta^a$	$\text{Im}\{\chi^{(3)}\}^b$	$\sigma_{Ex}/\sigma_g$	#	$\beta^a$	$\text{Im}\{\chi^{(3)}\}^b$	$\sigma_{Ex}/\sigma_g$
<b>H57</b> <sup>c,d</sup>	1.3	n.d.	5.7	<b>Sn60</b> <sup>e</sup>	3.9	396	9.62
<b>Sn57</b> <sup>d</sup>	2.9	n.d.	16.9	<b>Sn61</b> <sup>d</sup>	4.0	130	7.3
<b>H58</b> <sup>c</sup>	2.3	7.8	4.3	<b>Sn62</b> <sup>f</sup>	2.6	8.8	4.5
<b>Sn58</b> <sup>d</sup>	3.0	10.0	10.2	<b>Sn63</b> <sup>g</sup>	1.5	6.6	6.0
<b>Sn59</b> <sup>e</sup>	0.9	154	5.14	-	-	-	-

<sup>a</sup>  $\beta$  in  $10^{-8}$  cm $\cdot$ W $^{-1}$ , <sup>b</sup>  $\text{Im}\{\chi^{(3)}\}$  in  $10^{-12}$  esu <sup>c</sup> free base of **Sn57** or **Sn58**, <sup>d</sup> in THF, <sup>e</sup> in toluene, <sup>f</sup> in DMF, <sup>g</sup> in 1-chloronaphthalene.

In the case of the fully halogenated phthalocyanines, there is a noticeable trend when the axial ligand changes from chlorine (**Sn62**) to fluorine (**Sn63**), as in the porphyrins reported by Sing [88], this is related to the electronegativity of the ligands and the interaction of an even harder acid ( $F^-$ ) with a soft base ( $Sn^{IV}$ ). Not surprisingly, the best in this series is the perfluorinated phthalocyanine due to the well-known mesomeric effect of the fluorine in contrast to the inductive effect of the chlorine.

Organostannoxanes have also proved to be efficient for NLO. Tian et al. reported a series of organostannoxanes derived from phenothiazine [95], triphenylamine [96], coumarin [97] and cinnamic acid [98]. These compounds exhibit TPA values in the range of 680–850 nm, which are mostly part of the infrared region. In the solid state, the diphenyl tin derivatives usually remain as a discrete structure due to the bulky phenyl groups (Figure 52), however, for the dibutyl tin (Figure 53), it is very common to find them as dimeric [71,99], hexameric [100] or even 3D networks [101], as in the case of these organostannoxanes.

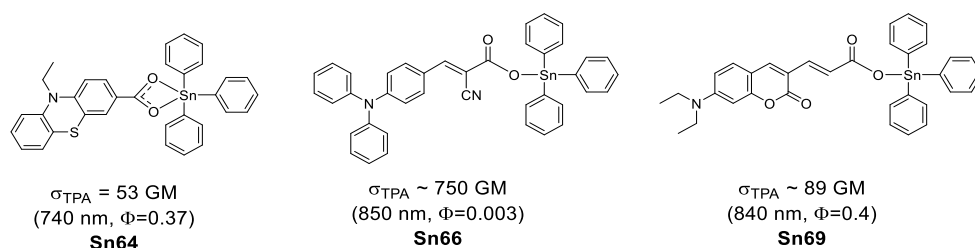


Figure 52. Some organostannoxanes with TPA properties.

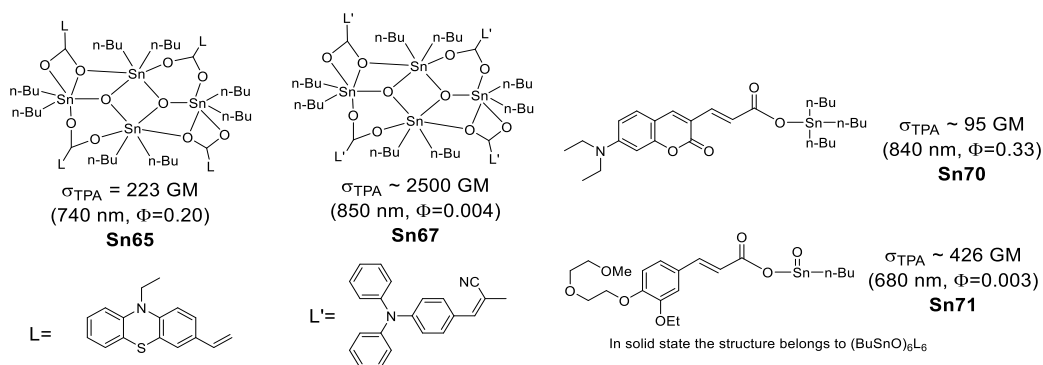


Figure 53. Some organostannoxanes with TPA properties.

Two-photon microscopy (TPM) has become a promising technique for biomedical research [102–105], Kim and Cho suggested that chromophores suitable for TPA applications should have (1) two-photon brightness ( $\sigma_{TPA} \times \Phi$ ) larger than 50 GM [103] or (2)  $\sigma_{TPA}/MW$  ( $GM \text{ g}^{-1} \cdot \text{mol}^{-1}$ ) larger than 1 [106].

Considering the above, only **Sn69** ( $61^a \text{ GM}$ ,  $89^b \text{ GM}$ ) and **Sn70** ( $69^b \text{ GM}$ ,  $95^c \text{ GM}$ ) meet the first requirement; the second requirement is fulfilled only by **Sn66** ( $1.06^b \text{ GM g}^{-1} \cdot \text{mol}^{-1}$ ), **Sn67** ( $1.93^b \text{ GM g}^{-1} \cdot \text{mol}^{-1}$ ), **Sn68** ( $2.64^b \text{ GM g}^{-1} \cdot \text{mol}^{-1}$ ), **Sn69** ( $3.83^c \text{ GM g}^{-1} \cdot \text{mol}^{-1}$ ) and **Sn70** ( $3.99^c \text{ GM g}^{-1} \cdot \text{mol}^{-1}$ ) (Table 8). This could make them suitable for bioimaging.

These compounds, as in other tin derivatives, also present biological activity; the derivatives from triphenylamine [96] are cytotoxic against A549 (lung cancer) and MDA-MB-231 (breast cancer) cell lines; the derivatives from coumarin [97] are active against Hela (cervical cancer), HepG2 (liver cancer), A549 and they proved to be better than cisplatin, inducing apoptosis by reactive oxygen species. The coumarin [107] derivative showed higher antibacterial activity against *Bacillus subtilis* than Kanamycin.

Li et al. [108] reported the study of tetrachloro (1,10-phenanthroline-*N,N'*) tin(IV) listed in Table 9 and their NLO properties.

**Table 8.** Optical properties of the organostannoxanes.

Tin complex	Tin Source	#	$\lambda_{\text{abs}}$ (nm)	$\lambda_{\text{em}}$ (nm)	#	$\sigma_{\text{TPA}}$ (GM)
Phenothiazine [95]	Ph <sub>3</sub> SnOH	<b>Sn64</b>	290, 363 <sup>a</sup>	537 <sup>a</sup>	0.37 <sup>a</sup>	53 <sup>a</sup>
	<i>n</i> -Bu <sub>2</sub> SnO	<b>Sn65</b>	302, 401 <sup>a</sup>	537 <sup>a</sup>	0.20 <sup>a</sup>	223 <sup>a</sup>
Triphenylamine [96]	Ph <sub>3</sub> SnOH	<b>Sn66</b>	289, 414 <sup>a</sup>	565 <sup>a</sup>	0.003 <sup>a</sup>	780 <sup>a</sup>
	<i>n</i> -Bu <sub>2</sub> SnO	<b>Sn67</b>	289, 426 <sup>a</sup>	553 <sup>a</sup>	0.004 <sup>a</sup>	2500 <sup>a</sup>
	( <i>n</i> -Bu <sub>3</sub> Sn) <sub>2</sub> O	<b>Sn68</b>	291, 419 <sup>a</sup>	556 <sup>a</sup>	0.008 <sup>a</sup>	1600 <sup>a</sup>
Coumarin [97,107]	Ph <sub>3</sub> SnOH	<b>Sn69</b>	449 <sup>b</sup> , 424 <sup>c</sup>	545 <sup>b</sup> , 485 <sup>c</sup>	0.025 <sup>b</sup> , 0.40 <sup>c</sup>	2440 <sup>b</sup> , 222 <sup>c</sup>
	( <i>n</i> -Bu <sub>3</sub> Sn) <sub>2</sub> O	<b>Sn70</b>	452 <sup>b</sup> , 431 <sup>c</sup>	547 <sup>b</sup> , 489 <sup>c</sup>	0.030 <sup>b</sup> , 0.33 <sup>c</sup>	2300 <sup>b</sup> , 287 <sup>c</sup>
Cinnamic acid [98]	<i>n</i> -BuSnOH	<b>Sn71</b>	321 <sup>d</sup>	410 <sup>d</sup>	0.009 <sup>d</sup>	426 <sup>d</sup>
	( <i>n</i> -Bu <sub>3</sub> Sn) <sub>2</sub> O	<b>Sn72</b>	320 <sup>d</sup>	406 <sup>d</sup>	0.003 <sup>d</sup>	-

<sup>a</sup> in CH<sub>2</sub>Cl<sub>2</sub>, <sup>b</sup> in phosphate buffered saline 0.02% triton X-100, <sup>c</sup> in DMF, <sup>d</sup> in DMSO.

**Table 9.** Optical properties of tetrachloro (1,10-phenanthroline-*N,N'*) tin(IV).

$\chi^{(3)}$	$3.6 \times 10^{-12}$ esu
$\text{Re}\{\chi^{(3)}\}$ <sup>a</sup>	$3.267 \times 10^{-12}$ esu
$\text{Im}\{\chi^{(3)}\}$	$1.512 \times 10^{-12}$ esu
$\Gamma$	$5.022 \times 10^{-33}$ esu
B	$3.18 \times 10^{-10}$ cm·W <sup>-1</sup>
$\eta_2$ <sup>b</sup>	$3.87 \times 10^{-22}$ esu

<sup>a</sup>  $\text{Re}\{\chi^{(3)}\}$  is the real part of the third order hyperpolarizability. <sup>b</sup>  $\eta_2$  is the nonlinear refraction index.

Diorganotin Schiff bases are another type of tin derivatives capable of third order NLO properties. Peon et al. [109] described a series of diphenyl tin(IV) Schiff bases (Figure 54), the fluorescence in these complexes are up to 50 times larger than the free base due to the rigidity imposed by the tin center.

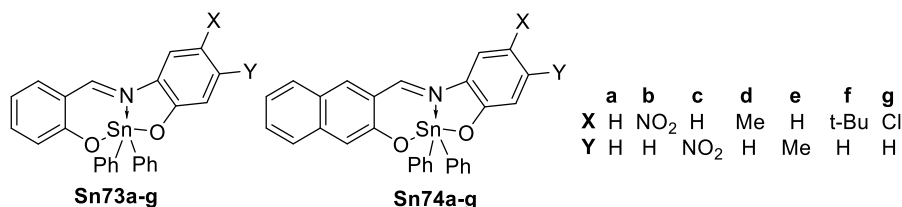


**Figure 54.** Diphenyl tin complexes reported by Peon et al. (Adapted with permission from [109]. Zugazagoitia, J.S.; Maya, M.; Damián-Zea, C.; Navarro, P.; Beltrán, H. I.; Peon, J. Excited-State Dynamics and Two-Photon Absorption Cross Sections of Fluorescent Diphenyl-Tin IV Derivatives with Schiff Bases: A Comparative Study of the Effect of Chelation from the Ultrafast to the Steady-State Time Scale. Copyright 2010 American Chemical Society.)

Increasing the conjugation of the system, should lead to a bathochromic shift in the UV-Vis and an increase in  $\sigma_{\text{TPA}}$ . As evident from Equation (4), decreasing the energy of the main transition associated to the TPA ( $E_{\text{ge}}$ ) normally should increase  $\sigma_{\text{TPA}}$ .

$$\sigma_{\text{TPA}} \approx \frac{16\pi^2 f (\mu_{\text{ee}} - \mu_{\text{gg}})^2}{5\hbar^2 c^2 \Gamma E_{\text{ge}}} \quad (4)$$

As expected, the naphthalene derivatives are red shifted in the UV-Vis spectra; also in both derivatives, large red shifts are observed when electron-donating groups are located at the *meta* position to the imino group, and with electron-withdrawing groups in the *para* position to the imino. On the other hand, when the electron-withdrawing group is *meta* to the imino a blue shift is observed.

The two-photon absorption spectra for diphenyl tin(IV) complexes were recorded in ethanol (Figure 55). As expected the naphthalene series shows larger  $\sigma_{\text{TPA}}$ , indeed the largest in each series is observed for **Sn73c** and **Sn74c** (nitro group *para* to the imino) and **Sn74d** (methyl *meta* to the imino).

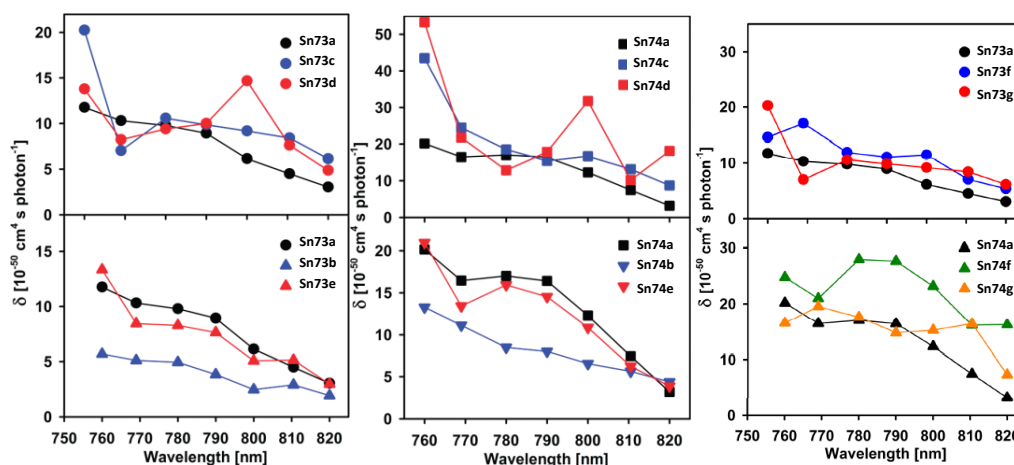


**Figure 55.** TPA spectra for diphenyl tin(IV) complexes **Sn73a–g** and **Sn74a–g**, (Adapted with permission from [109], Zugazagoitia, J.S.; Maya, M.; Damián-Zea, C.; Navarro, P.; Beltrán, H. I.; Peon, J. Excited-State Dynamics and Two-Photon Absorption Cross Sections of Fluorescent Diphenyl-Tin IV Derivatives with Schiff Bases: A Comparative Study of the Effect of Chelation from the Ultrafast to the Steady-State Time Scale. Copyright 2010 American Chemical Society.)

Muñoz-Flores et al. [110] reported four organotin Schiff compounds with “push-pull” architecture as depicted in Figure 56. The diphenyl tin complexes were thermally more stable than the dibutyl tin complexes, and their decomposition follows the order  $T_0$ : 227 °C (**Sn75**) > 171 °C (**Sn77**) > 96 °C (**Sn76**) > 95 °C (**Sn78**). The optical properties were obtained for the different tin complexes in spin-coated polymer films; the UV–Vis spectra of the diethylamino derivatives show a bathochromic shift of about 30 nm with respect to the methoxy derivatives, in full agreement with a better electron-donating capability of the former group. The values observed for  $\chi^{(3)}$  (Table 10) follow the same trend for the electron-donating capabilities and are in the same order of magnitude obtained for previous tin complexes.

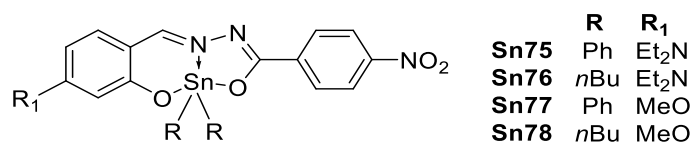


**Figure 56.** Diphenyl tin complexes reported by Muñoz-Flores et al. (Reprinted from [110], García-López, M.C.; Muñoz-Flores, B.M.; Chan-Navarro, R.; Jiménez-Pérez, V.M.; Moggio, I.; Arias, E.; Rodríguez-Ortega, A.; Ochoa, M.E. Microwave-assisted synthesis, third-order nonlinear optical properties, voltammetry cyclic and theoretical calculations of organotin compounds bearing push-pull Schiff bases. Copyright 2016, with permission from Elsevier).

**Table 10.** Third order susceptibilities for **Sn75–78**.

#	$\chi^{(3)} \times 10^{-12}$ esu
<b>Sn75</b>	3.18
<b>Sn76</b>	3.02
<b>Sn77</b>	1.38
<b>Sn78</b>	1.43

A series of diorganotin Schiff bases derived from fluorene (Figure 57) was reported by Farfán et al. [111], as in the case of other compounds, the fluorene was introduced to enhance the TPA response [112–114]. These complexes showed no response to the polarity of the solvent and moderate fluorescence quantum yields.

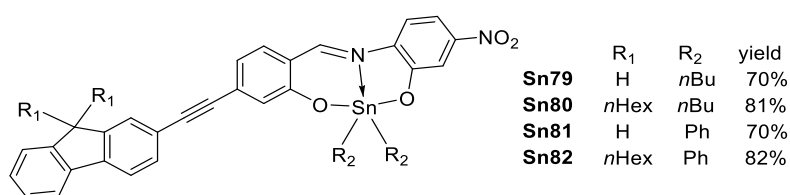


**Figure 57.** Diorganotin complexes derived from fluorene.

The TPA spectra for **Sn80** was recorded in DMSO, THF and CHCl<sub>3</sub> (Table 11). Although the maximum was found at around 750 nm in the three solvents, in chloroform the TPA response is enhanced (Figure 58) and it is possible to observe a second absorption at 1000 nm that is roughly observed in DMSO and THF. This is explained because the two-photon excitation fluorescence comes from the lowest excited state S<sub>1</sub> [48] as reported by Peon for this type of complex [109]. In this case, the excited state is accessible through excitation at the bands located around 400 nm and 500 nm in the OPA spectra explaining the presence of the second band.

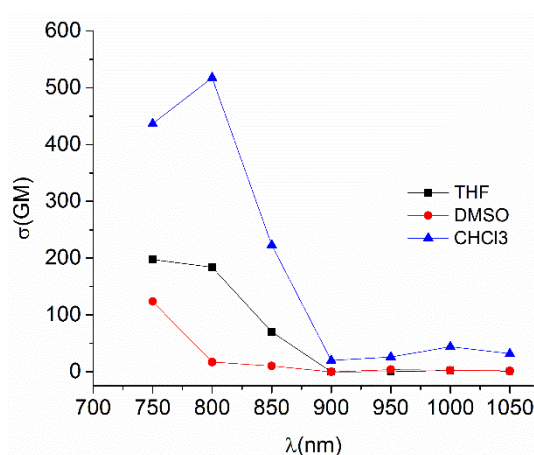


**Figure 58.** TPA spectra for **Sn80** in different solvents.

The complex **Sn80** has the largest  $\sigma_{TPA}$  (517 GM) of the four derivatives, and of previously diorganotin Schiff bases. Furthermore, its two-photon brightness ( $\sigma_{TPA} \times \Phi$ ) is of 150 GM which makes it the best organotin complex suitable for two-photon microscopy (excluding porphyrins or phthalocyanines tin complexes, which show exceptional TPA responses).

**Table 11.** Largest TPA observed in chloroform for **Sn79–Sn82**.

#	$\sigma_{TPA}$ (GM)
<b>Sn79</b>	440
<b>Sn80</b>	517
<b>Sn81</b>	355
<b>Sn82</b>	188

**Author Contributions:** C.C.J. has written section 2.1. “Second Order NLO for boron compounds”, O.G.-A. has written Section 2.2. “Third Order NLO for boron compounds”, J.O.-H. and P.L.-V. have written Section 3.1. “Second Order NLO for tin compounds”, A.E.-C. has written Section 3.2. “Third Order NLO for boron compounds”, N.F. and R.S. and P.G.L have critically and scientifically revised the original. All authors contributed to the final revision.

**Funding:** The authors thank CNRS (France), PAIP, PAPIIT IN216616 (UNAM). This work has been realized within the framework of the French-Mexican international laboratory (LIA-LCMMC).

**Acknowledgments:** The following authors thank CONACyT for the PhD grant: O.G.-A. (239984), A.E.-C. (270200), J.O.-H. (271117) and P.L.-V. (337958).

**Conflicts of Interest:** The authors declare no conflict of interest.

## References

1. Suresh, S.; Ramanand, A.; Jayaraman, D.; Mani, P. Review on theoretical aspect of nonlinear optics. *Rev. Adv. Mater. Sci.* **2012**, *30*, 175–183. [\[CrossRef\]](#)
2. Maiman, T.H. Optical MASER action in ruby. *Br. Commun. Electron.* **1960**, *7*.
3. Maiman, T.H. Stimulated Optical Radiation in Ruby. *Nature* **1960**, *187*, 493–494. [\[CrossRef\]](#)
4. Franken, P.A.; Hill, A.E.; Peters, C.W.; Weinreich, G. Generation of Optical Harmonics. *Phys. Rev. Lett.* **1961**, *7*, 118–119. [\[CrossRef\]](#)
5. Hosmane, N.S. Chapter13: Boron Derivatives for Application in Nonlinear Optics. In *Boron Science: New Technologies and Applications*; CRC Press: Boca Raton, FL, USA, 2012; pp. 295–317. ISBN 978-1-4398-2663-8.
6. Rentzepis, P.M.; Pao, Y. Laser-Induced Optical Second Harmonic Generation in Organic Crystals. *Appl. Phys. Lett.* **1964**, *5*, 156–158. [\[CrossRef\]](#)
7. Buckingham, A.D.; Clarke, K.L. Long-range effects of molecular interactions on the polarizability of atoms. *Chem. Phys. Lett.* **1978**, *57*, 321–325. [\[CrossRef\]](#)
8. Stahl, R.; Lambert, C.; Kaiser, C.; Wortmann, R.; Jakober, R. Electrochemistry and photophysics of donor-substituted triarylboranes: Symmetry breaking in ground and excited state. *Chem. Eur. J.* **2006**, *12*, 2358–2370. [\[CrossRef\]](#)
9. Kurtz, S.K.; Perry, T.T. A Powder Technique for the Evaluation of Nonlinear Optical Materials. *J. Appl. Phys.* **1968**, *39*, 3798–3813. [\[CrossRef\]](#)
10. Oudar, J.L. Optical nonlinearities of conjugated molecules. Stilbene derivatives and highly polar aromatic compounds. *J. Chem. Phys.* **1977**, *67*, 446–457. [\[CrossRef\]](#)
11. Kanis, D.R.; Ratner, M.A.; Marks, T.J.; Zerner, M.C. Nonlinear Optical Characteristics of Novel Inorganic Chromophores Using the Zindo Formalism. *Chem. Mater.* **1991**, *3*, 19–22. [\[CrossRef\]](#)
12. Kanis, D.R.; Ratner, M.A.; Marks, T.J. Design and Construction of Molecular Assemblies with Large Second-Order Optical Nonlinearities. Quantum Chemical Aspects. *Chem. Rev.* **1994**, *94*, 195–242. [\[CrossRef\]](#)
13. Ledoux, I.; Zyss, J. Influence of the molecular environment in solution measurements of the Second-order optical susceptibility for urea and derivatives. *Chem. Phys.* **1982**, *73*, 203–213. [\[CrossRef\]](#)
14. Eaton, D.F. Nonlinear Optical Materials. *Science* **1991**, *253*, 281–287. [\[CrossRef\]](#) [\[PubMed\]](#)
15. Meyers, F.; Marder, S.R.; Pierce, B.M.; Bredas, J.L. Electric Field Modulated Nonlinear Optical Properties of Donor–Acceptor Polyenes: Sum-Over-States Investigation of the Relationship between Molecular Polarizabilities ( $\alpha$ ,  $\beta$ , and  $\gamma$ ) and Bond Length Alternation. *J. Am. Chem. Soc.* **1994**, *116*, 10703–10714. [\[CrossRef\]](#)
16. Pawlicki, M.; Collins, H.A.; Denning, R.G.; Anderson, H.L. Two-Photon Absorption and the Design of Two-Photon Dyes. *Angew. Chem. Int. Ed.* **2009**, *48*, 3244–3266. [\[CrossRef\]](#) [\[PubMed\]](#)
17. Neckers, D.C.; Jenks, W.S.; Wolff, T. (Eds.) *Advances in Photochemistry*; John Wiley & Sons, Inc.: Hoboken, NJ, USA, 2006; ISBN 9780470037584.
18. Andraud, C.; Fortrie, R.; Barsu, C.; Stéphan, O.; Chermette, H.; Baldeck, P.L. Excitonically Coupled Oligomers and Dendrimers for Two-Photon Absorption. In *Photoresponsive Polymers II*; Springer: Berlin/Heidelberg, Germany, 2008; Volume 214, pp. 149–203. ISBN 9783540694526.
19. Wakamiya, A.; Yamaguchi, S. Designs of functional  $\pi$ -electron materials based on the characteristic features of boron. *Bull. Chem. Soc. Jpn.* **2015**, *88*, 1357–1377. [\[CrossRef\]](#)
20. Grisdale, P.J.; Williams, J.L.R.; Glogowski, M.E.; Babb, B.E. Boron Photochemistry. VI. The Possible Role of Bridged Intermediates in the Photolysis of Borate Complexes. *J. Org. Chem.* **1971**, *36*, 544–549. [\[CrossRef\]](#)
21. Doty, J.C.; Babb, B.; Grisdale, P.J.; Glogowski, M.; Williams, J.L.R. Donor Acceptor Boron Nitrogen. *J. Organomet. Chem.* **1972**, *38*, 229–236. [\[CrossRef\]](#)
22. Yuan, Z.; Taylor, N.J.; Marder, T.B.; Williams, I.D.; Kurtz, S.K.; Cheng, L.-T. Three coordinate phosphorus and boron as  $\pi$ -donor and  $\pi$ -acceptor moieties respectively, in conjugated organic molecules for nonlinear optics: Crystal and molecular structures of *E*-Ph-CH=CH-B(mes)<sub>2</sub>, *E*-4-MeO-C<sub>6</sub>H<sub>4</sub>-CH=CH-B(mes)<sub>2</sub>, and *E*-Ph<sub>2</sub>P-CH=CH-B(mes)<sub>2</sub> [mes = 2,4,6-Me<sub>3</sub>C<sub>6</sub>H<sub>2</sub>]. *J. Chem. Soc. Chem. Commun.* **1990**, *2*, 1489–1492. [\[CrossRef\]](#)
23. Lequan, M.; Lequan, R.M.; Ching, K.C. Trivalent Boron as acceptor chromophore in asymmetrically substituted 4,4'-biphenyl and azobenzene for non-linear optics. *J. Mater. Chem.* **1991**, *1*, 997–999. [\[CrossRef\]](#)

24. Singer, K.D.; Garito, A.F. Measurements of molecular second order optical susceptibilities using dc induced second harmonic generation. *J. Chem. Phys.* **1981**, *75*, 3572–3580. [[CrossRef](#)]
25. Yuan, Z.; Taylor, N.J.; Sun, Y.; Marder, T.B.; Williams, I.D.; Cheng, L.-T. Synthesis and second-order nonlinear optical properties of three coordinate organoboranes with diphenylphosphino and ferrocenyl groups as electron donors: Crystal and molecular structures of (E)-D-CH=CH-B(mes)<sub>2</sub>, and D-C=C-B(mes)<sub>2</sub>, [D = P(C<sub>6</sub>H<sub>5</sub>)<sub>2</sub>, (η-C<sub>5</sub>H<sub>5</sub>)Fe(η-C<sub>5</sub>H<sub>4</sub>); mes = 2,4,6-(CH<sub>3</sub>)<sub>3</sub>C<sub>6</sub>H<sub>2</sub>]. *J. Organomet. Chem.* **1993**, *449*, 27–37. [[CrossRef](#)]
26. Branger, C.; Lequan, M.; Lequan, R.M.; Barzoukas, M.; Fort, A. Boron derivatives containing a bithiophene bridge as new materials for non-linear optics. *J. Mater. Chem.* **1996**, *6*, 555. [[CrossRef](#)]
27. Branger, C.; Lequan, M.; Lequan, R.M.; Large, M.; Kajzar, F. Polyurethanes containing boron chromophores as sidechains for nonlinear optics. *Chem. Phys. Lett.* **1997**, *272*, 265–270. [[CrossRef](#)]
28. Lesley, M.J.G.; Woodward, A.; Taylor, N.J.; Marder, T.B.; Cazenobe, I.; Ledoux, I.; Zyss, J.; Thornton, A.; Bruce, D.W.; Kakkar, A.K. Lewis Acidic Borane Adducts of Pyridines and Stilbazoles for Nonlinear Optics. *Chem. Mater.* **1998**, *10*, 1355–1365. [[CrossRef](#)]
29. Su, Z.M.; Wang, X.J.; Huang, Z.H.; Wang, R.S.; Feng, J.K.; Sun, J.Z. Nonlinear optical properties for pyridines and stilbazoles adducted by borane. *Synth. Met.* **2001**, *119*, 583–584. [[CrossRef](#)]
30. Reyes, H.; Muñoz, B.M.; Farfán, N.; Santillan, R.; Rojas-Lima, S.; Lacroix, P.G.; Nakatani, K. Synthesis, crystal structures, and quadratic nonlinear optical properties in a series of push-pull boronate derivatives. *J. Mater. Chem.* **2002**, *12*, 2898–2903. [[CrossRef](#)]
31. Entwistle, C.D.; Marder, T.B. Boron Chemistry Lights the Way: Optical Properties of Molecular and Polymeric Systems. *Angew. Chem. Int. Ed.* **2002**, *41*, 2927. [[CrossRef](#)]
32. Entwistle, C.D.; Marder, T.B. Applications of Three-Coordinate Organoboron Compounds and Polymers in Optoelectronics. *Chem. Mater.* **2004**, *16*, 4574–4585. [[CrossRef](#)]
33. Yamaguchi, S.; Wakamiya, A. Boron as a key component for new π-electron materials. *Pure Appl. Chem.* **2006**, *78*. [[CrossRef](#)]
34. Lamère, J.F.; Lacroix, P.G.; Farfán, N.; Rivera, J.M.; Santillan, R.; Nakatani, K. Synthesis, characterization and nonlinear optical (NLO) properties of a push-pull bisboronate chromophore with a potential electric field induced NLO switch. *J. Mater. Chem.* **2006**, *16*, 2913–2920. [[CrossRef](#)]
35. Muñoz, B.M.; Santillan, R.; Rodríguez, M.; Méndez, J.M.; Romero, M.; Farfán, N.; Lacroix, P.G.; Nakatani, K.; Ramos-Ortiz, G.; Maldonado, J.L. Synthesis, crystal structure and non-linear optical properties of boronates derivatives of salicylideniminophenols. *J. Organomet. Chem.* **2008**, *693*, 1321–1334. [[CrossRef](#)]
36. Rodríguez, M.; Maldonado, J.L.; Ramos-Ortiz, G.; Lamère, J.F.; Lacroix, P.G.; Farfán, N.; Ochoa, M.E.; Santillan, R.; Meneses-Nava, M.A.; Barbosa-García, O.; Nakatani, K. Synthesis and non-linear optical characterization of novel borinate derivatives of cinnamaldehyde. *New J. Chem.* **2009**, *33*, 1693–1702. [[CrossRef](#)]
37. Zhang, Z.; Edkins, R.M.; Nitsch, J.; Fücke, K.; Eichhorn, A.; Steffen, A.; Wang, Y.; Marder, T.B. D-π-A triarylboron compounds with tunable push-pull character achieved by modification of both the donor and acceptor moieties. *Chem. Eur. J.* **2015**, *21*, 177–190. [[CrossRef](#)]
38. Ji, L.; Griesbeck, S.; Marder, T.B. Recent developments in and perspectives on three-coordinate boron materials: A bright future. *Chem. Sci.* **2017**, *8*, 846–863. [[CrossRef](#)] [[PubMed](#)]
39. Gao, S.M.; Hosmane, N.S. Dendrimer- and nanostructure-supported carboranes and metallacarboranes: An account. *Russ. Chem. Bull.* **2014**, *63*, 788–810. [[CrossRef](#)]
40. Núñez, R.; Tarrés, M.; Ferrer-Ugalde, A.; de Biani, F.F.; Teixidor, F. Electrochemistry and Photoluminescence of Icosahedral Carboranes, Boranes, Metallacarboranes, and Their Derivatives. *Chem. Rev.* **2016**, *116*, 14307–14378. [[CrossRef](#)] [[PubMed](#)]
41. Ma, N.N.; Li, S.J.; Yan, L.K.; Qiu, Y.Q.; Su, Z.M. Switchable NLO response induced by rotation of metallacarboranes [NiIII/IV(C<sub>2</sub>B<sub>9</sub>H<sub>11</sub>)<sub>2</sub>]<sup>−/0</sup> and C-, B-functionalized derivatives. *Dalton Trans.* **2014**, *43*, 5069–5075. [[CrossRef](#)]
42. Gassin, P.M.; Girard, L.; Martin-Gassin, G.; Brusselle, D.; Jonchère, A.; Diat, O.; Viñas, C.; Teixidor, F.; Bauduin, P. Surface activity and molecular organization of metallacarboranes at the air-water interface revealed by nonlinear optics. *Langmuir* **2015**, *31*, 2297–2303. [[CrossRef](#)]
43. Lequan, M.; Lequan, R.M.; Chane-ching, K.; Callier, A.; Barzoukas, M.; Fort, A. Second-Order optical non-linearities of {4-(dimethylamino) stilben Z & E 4'-yl} dimesityl borane. *Adv. Mater. Opt. Electron.* **1992**, *1*, 243–247. [[CrossRef](#)]

44. Vondung, L.; Alig, L.; Ballmann, M.; Langer, R. Umpolung at Boron: Ancillary-Ligand-Induced Formation of Boron-Based Donor Ligands from Phosphine-Boranes. *Chem. Eur. J.* **2018**, *24*, 12346–12353. [[CrossRef](#)] [[PubMed](#)]
45. Lambert, C.; Stadler, S.; Bourhill, G.; Bräuchle, C. Polarized  $\pi$ -Electron Systems in a Chemically Generated Electric Field: Second-Order Nonlinear Optical Properties of Ammonium/Borate Zwitterions. *Angew. Chem. Int. Ed.* **1996**, *35*, 644–646. [[CrossRef](#)]
46. Reinhardt, B.A.; Brott, L.L.; Clarson, S.J.; Dillard, A.G.; Bhatt, J.C. Highly Active Two-Photon Dyes: Design, Synthesis, and Characterization toward Application. *Chem. Mater.* **1998**, *38*, 1863–1874. [[CrossRef](#)]
47. Yuan, Z.; Taylor, N.J.; Ramachandran, R.; Marder, T.B. Third-order nonlinear optical properties of organoboron compounds: Molecular structures and second hyperpolarizabilities. *Appl. Organomet. Chem.* **1996**, *10*, 305–316. [[CrossRef](#)]
48. Albota, M. Design of Organic Molecules with Large Two-Photon Absorption Cross Sections. *Science* **1998**, *281*, 1653–1656. [[CrossRef](#)] [[PubMed](#)]
49. Belfield, K.D.; Hagan, D.J.; Van Stryland, E.W.; Schafer, K.J.; Negres, R.A. New Two-Photon Absorbing Fluorene Derivatives: Synthesis and Nonlinear Optical Characterization. *Org. Lett.* **1999**, *1*, 1575–1578. [[CrossRef](#)]
50. Matsumi, N.; Chujo, Y. A new class of p-conjugated organoboron polymers. In *Contemporary Boron Chemistry*; Davidson, M.G., Wade, K., Marder, T.B., Hughes, A.K., Eds.; The Royal Society of Chemistry: Cambridge, UK, 2000; pp. 51–58. ISBN 978-0-85404-835-9.
51. Liu, Z.; Fang, Q.; Wang, D.; Xue, G.; Yu, W.; Shao, Z.; Jiang, M. Trivalent boron as acceptor in D- $\pi$ -A chromophores: Synthesis, structure and fluorescence following single- and two-photon excitation. *Chem. Commun.* **2002**, 2900–2901. [[CrossRef](#)]
52. Liu, Z.; Fang, Q.; Wang, D.; Cao, D.; Xue, G.; Yu, W.; Lei, H. Trivalent Boron as an Acceptor in Donor- $\pi$ -Acceptor-Type Compounds for Single- and Two-Photon Excited Fluorescence. *Chem. Eur. J.* **2003**, *9*, 5074–5084. [[CrossRef](#)]
53. Liu, Z.-Q.; Fang, Q.; Cao, D.-X.; Wang, D.; Xu, G.-B. Triaryl Boron-Based A- $\pi$ -A vs. Triaryl Nitrogen-Based D- $\pi$ -D Quadrupolar Compounds for Single- and Two-Photon Excited Fluorescence. *Org. Lett.* **2004**, *6*, 2933–2936. [[CrossRef](#)]
54. Tao, L.-M.; Guo, Y.-H.; Huang, X.-M.; Wang, C.-K. Theoretical studies on two-photon absorption properties of newly synthesized triaryl boron-based A- $\pi$ -A and triaryl nitrogen-based D- $\pi$ -D quadrupolar compounds. *Chem. Phys. Lett.* **2006**, *425*, 10–15. [[CrossRef](#)]
55. Halik, M.; Wenseleers, W.; Grasso, C.; Stellacci, F.; Zojer, E.; Barlow, S.; Brédas, J.-L.; Perry, J.W.; Marder, S.R. Bis(dioxaborine) compounds with large two-photon cross sections, and their use in the photodeposition of silver. *Chem. Commun.* **2003**, *3*, 1490–1491. [[CrossRef](#)]
56. Cogné-Laage, E.; Allemand, J.-F.; Ruel, O.; Baudin, J.-B.; Croquette, V.; Blanchard-Desce, M.; Jullien, L. Diaryl(methanato)boron Difluoride Compounds as Medium-Sensitive Two-Photon Fluorescent Probes. *Chem. Eur. J.* **2004**, *10*, 1445–1455. [[CrossRef](#)] [[PubMed](#)]
57. Yuan, Z.; Entwistle, C.D.; Collings, J.C.; Albesa-Jové, D.; Batsanov, A.S.; Howard, J.A.K.; Taylor, N.J.; Kaiser, H.M.; Kaufmann, D.E.; Poon, S.-Y.; et al. Synthesis, Crystal Structures, Linear and Nonlinear Optical Properties, and Theoretical Studies of (*p*-R-Phenyl)-, (*p*-R-Phenylethynyl)-, and (*E*)-[2-(*p*-R-Phenyl)ethenyl]dimesitylboranes and Related Compounds. *Chem. Eur. J.* **2006**, *12*, 2758–2771. [[CrossRef](#)] [[PubMed](#)]
58. Hayek, A.; Nicoud, J.-F.; Bolze, F.; Bourgogne, C.; Baldeck, P.L. Boron-Containing Two-Photon-Absorbing Chromophores: Electronic Interaction through the Cyclodiborazane Core. *Angew. Chem. Int. Ed.* **2006**, *45*, 6466–6469. [[CrossRef](#)] [[PubMed](#)]
59. Hayek, A.; Bolze, F.; Bourgogne, C.; Baldeck, P.L.; Didier, P.; Arntz, Y.; Mély, Y.; Nicoud, J.-F. Boron Containing Two-Photon Absorbing Chromophores. 2. Fine Tuning of the One- and Two-Photon Photophysical Properties of Pyrazabole Based Fluorescent Bioprobes. *Inorg. Chem.* **2009**, *48*, 9112–9119. [[CrossRef](#)] [[PubMed](#)]
60. Nicoud, J.-F.; Bolze, F.; Sun, X.-H.; Hayek, A.; Baldeck, P. Boron-Containing Two-Photon-Absorbing Chromophores. 3.(1) One- and Two-Photon Photophysical Properties of p -Carborane-Containing Fluorescent Bioprobes. *Inorg. Chem.* **2011**, *50*, 4272–4278. [[CrossRef](#)]

61. Rodríguez, M.; Castro-Beltrán, R.; Ramos-Ortiz, G.; Maldonado, J.L.; Farfán, N.; Domínguez, O.; Rodríguez, J.; Santillan, R.; Meneses-Nava, M.A.; Barbosa-García, O.; Peon, J. Synthesis and third-order nonlinear optical studies of a novel four-coordinated organoboron derivative and a bidentate ligand. *Synth. Met.* **2009**, *159*, 1281–1287. [[CrossRef](#)]
62. Li, H.-J.; Fu, W.-F.; Li, L.; Gan, X.; Mu, W.-H.; Chen, W.-Q.; Duan, X.-M.; Song, H.-B. Intense One- and Two-Photon Excited Fluorescent Bis(BF<sub>2</sub>) Core Complex Containing a 1,8-Naphthyridine Derivative. *Org. Lett.* **2010**, *12*, 2924–2927. [[CrossRef](#)] [[PubMed](#)]
63. Jadhav, T.; Maragani, R.; Misra, R.; Sreeramulu, V.; Rao, D.N.; Mobin, S.M. Design and synthesis of donor–acceptor pyrazobole derivatives for multiphoton absorption. *Dalton Trans.* **2013**, *42*, 4340. [[CrossRef](#)]
64. D’Aléo, A.; Felouat, A.; Fages, F. Boron difluoride complexes of 2'-hydroxychalcones and curcuminoids as fluorescent dyes for photonic applications. *Adv. Nat. Sci. Nanosci. Nanotechnol.* **2015**, *6*. [[CrossRef](#)]
65. Lanoë, P.-H.; Mettra, B.; Liao, Y.Y.; Calin, N.; D’Aléo, A.; Namikawa, T.; Kamada, K.; Fages, F.; Monnereau, C.; Andraud, C. Theoretical and Experimental Study on Boron  $\beta$ -Diketonate Complexes with Intense Two-Photon-Induced Fluorescence in Solution and in the Solid State. *ChemPhysChem* **2016**, *17*, 2128–2136. [[CrossRef](#)] [[PubMed](#)]
66. Kamada, K.; Namikawa, T.; Senatore, S.; Matthews, C.; Lenne, P.F.; Maury, O.; Andraud, C.; Ponce-Vargas, M.; Le Guennic, B.; Jacquemin, D.; et al. Boron Difluoride Curcuminoid Fluorophores with Enhanced Two-Photon Excited Fluorescence Emission and Versatile Living-Cell Imaging Properties. *Chem. Eur. J.* **2016**, *22*, 5219–5232. [[CrossRef](#)] [[PubMed](#)]
67. Lamberth, C.; Machell, J.C.; Mingos, D.M.P.; Stolberg, T.L. Preparation and 2nd harmonic generation properties of tris(pyrocatecholato)stannate(IV) compounds. *J. Mater. Chem.* **1991**, *1*, 775–780. [[CrossRef](#)]
68. Lequan, M.; Branger, C.; Simon, J.; Thami, T.; Chauchard, E.; Persoons, A. Hyperpolarizability of tetraorganotin compounds determined by the hyper-Rayleigh scattering technique. *Chem. Phys. Lett.* **1994**, *229*, 101–104. [[CrossRef](#)]
69. Lequan, M.; Branger, C.; Simon, J.; Thami, T.; Chauchard, E.; Persoons, A. First hyperpolarizability of organotin compounds with Td symmetry. *Adv. Mater.* **1994**, *6*, 851–853. [[CrossRef](#)]
70. Fiorini, C.; Nunzi, J.M.; Raimond, P.; Branger, C.; Lequan, M.; Lequan, R.M. Symmetry of the all-optical orientation dynamics of an octupolar azo-dye salt. *Synth. Met.* **2000**, *115*, 127–131. [[CrossRef](#)]
71. Reyes, H.; García, C.; Farfán, N.; Santillan, R.; Lacroix, P.G.; Lepetit, C.; Nakatani, K. Syntheses, crystal structures, and quadratic nonlinear optical properties in four “push-pull” diorganotin derivatives. *J. Organomet. Chem.* **2004**, *689*, 2303–2310. [[CrossRef](#)]
72. Guan, W.; Yang, G.; Yan, L.; Su, Z. Prediction of second-order optical nonlinearity of trisorganotin-substituted  $\beta$ -Keggin polyoxotungstate. *Inorg. Chem.* **2006**, *45*, 7864–7868. [[CrossRef](#)]
73. Rivera, J.M.; Guzmán, D.; Rodríguez, M.; Lamère, J.F.; Nakatani, K.; Santillan, R.; Lacroix, P.G.; Farfán, N. Synthesis, characterization and nonlinear optical properties in a series of new chiral organotin(IV) Schiff base complexes. *J. Organomet. Chem.* **2006**, *691*, 1722–1732. [[CrossRef](#)]
74. Rivera, J.M.; Reyes, H.; Cortés, A.; Santillan, R.; Lacroix, P.G.; Lepetit, C.; Nakatani, K.; Farfán, N. Second-Harmonic Generation within the P<sub>2</sub>1<sub>2</sub>1<sub>2</sub> Space Group, in a Series of Chiral (Salicylaldiminato) tin Schiff Base Complexes. *Chem. Mater.* **2006**, *18*, 1174–1183. [[CrossRef](#)]
75. Kumar, A.; Prasad, R.; Kociok-Köhn, G.; Molloy, K.C.; Singh, N. Synthesis, structure and calculated NLO properties of [(n-Bu)<sub>2</sub>Sn- $\mu$ -O- $\mu$ -OH-Sn(n-Bu)<sub>2</sub>(CH<sub>3</sub>CO<sub>2</sub>)<sub>2</sub>]<sub>2</sub> and its putative derivatives. *Inorg. Chem. Commun.* **2009**, *12*, 686–690. [[CrossRef](#)]
76. Muñoz-Flores, B.M.; Santillán, R.; Farfán, N.; Álvarez-Venicio, V.; Jiménez-Pérez, V.M.; Rodríguez, M.; Morales-Saavedra, O.G.; Lacroix, P.G.; Lepetit, C.; Nakatani, K. Synthesis, X-ray diffraction analysis and nonlinear optical properties of hexacoordinated organotin compounds derived from Schiff bases. *J. Organomet. Chem.* **2014**, *769*, 64–71. [[CrossRef](#)]
77. Şirikci, G.; Ancin, N.A.; Öztas, S.G. Theoretical studies of organotin(IV) complexes derived from ONO-donor type schiff base ligands. *J. Mol. Model.* **2015**, *21*. [[CrossRef](#)] [[PubMed](#)]
78. Dey, D.K.; Dey, S.P.; Karan, N.K.; Datta, A.; Lycka, A.; Rosair, G.M. Structural and spectral studies of 3-(2-hydroxyphenylimino)-1-phenylbutan-1-one and its diorganotin(IV) complexes. *J. Organomet. Chem.* **2009**, *694*, 2434–2441. [[CrossRef](#)]

79. Öztaş, N.A.; Yenişehirli, G.; Ancin, N.; Öztaş, S.G.; Özcan, Y.; Ide, S. Synthesis, characterization, biological activities of dimethyltin(IV) complexes of Schiff bases with ONO-type donors. *Spectrochim. Acta A* **2009**, *72*, 929–935. [[CrossRef](#)] [[PubMed](#)]
80. Yenişehirli, G.; Öztaş, N.A.; Şahin, E.; Çelebier, M.; Ancin, N.; Öztaş, S.G. Synthesis, characterization, and in vitro antimicrobial activities of organotin(IV) complexes of Schiff bases with ONO-type donor atoms. *Heteroat. Chem.* **2010**, *21*, 373–385. [[CrossRef](#)]
81. Öztaş, S.G.; Şahin, E.; Ancin, N.; Ide, S.; Tüzün, M. Structural and spectral studies of *N*-(3-hydroxypyridine-2-yl)-5-hydroxysalicylideneimine and its dimethyltin(IV) complex. *J. Mol. Struct.* **2004**, *705*, 107–112. [[CrossRef](#)]
82. Rosemann, N.W.; Eußner, J.P.; Dornsiepen, E.; Chatterjee, S.; Dehnen, S. Organotetrel Chalcogenide Clusters: Between Strong Second-Harmonic and White-Light Continuum Generation. *J. Am. Chem. Soc.* **2016**, *138*, 16224–16227. [[CrossRef](#)]
83. Rosemann, N.W.; Eussner, J.P.; Beyer, A.; Koch, S.W.; Volz, K.; Dehnen, S.; Chatterjee, S. A highly efficient directional molecular white-light emitter driven by a continuous-wave laser diode. *Science* **2016**, *352*, 1301–1304. [[CrossRef](#)]
84. Nakel, W. The elementary process of bremsstrahlung. *Phys. Rep.* **1994**, *243*, 317–353. [[CrossRef](#)]
85. Haug, E.; Nakel, W. *The Elementary Process of Bremsstrahlung*; Lecture Notes in Physics; World Scientific Lecture Notes; World Scientific, Toh Tuck Link: Singapore, 2004; Volume 73, ISBN 978-981-238-578-9.
86. Dang, Y.; Zhong, C.; Zhang, G.; Ju, D.; Wang, L.; Xia, S.; Xia, H.; Tao, X. Crystallographic Investigations into Properties of Acentric Hybrid Perovskite Single Crystals  $\text{NH}(\text{CH}_3)_3\text{SnX}_3$  ( $\text{X} = \text{Cl}, \text{Br}$ ). *Chem. Mater.* **2016**, *28*, 6968–6974. [[CrossRef](#)]
87. Eckardt, R.; Reintjes, J. Phase matching limitations of high efficiency second harmonic generation. *IEEE J. Quantum Electron.* **1984**, *20*, 1178–1187. [[CrossRef](#)]
88. Kandasamy, K.; Shetty, S.J.; Puntambekar, P.N.; Srivastava, T.S.; Kundu, T.; Singh, B.P. Effects of Metal Substitution on Third-order Optical Non-linearity of Porphyrin Macrocyclic. *J. Porphyr. Phthalocyanines* **1999**, *3*, 81–86. [[CrossRef](#)]
89. Kiran, P.P.; Reddy, D.R.; Dharmadhikari, A.K.; Maiya, B.G.; Kumar, G.R.; Rao, D.N. Contribution of two-photon and excited state absorption in “axial-bonding” type hybrid porphyrin arrays under resonant electronic excitation. *Chem. Phys. Lett.* **2006**, *418*, 442–447. [[CrossRef](#)]
90. Kiran, P.P.; Reddy, D.R.; Maiya, B.G.; Dharmadhikari, A.K.; Kumar, G.R.; Rao, D.N. Nonlinear absorption properties of “axial-bonding” type tin(IV) tetratolylporphyrin based hybrid porphyrin arrays. *Opt. Commun.* **2005**, *252*, 150–161. [[CrossRef](#)]
91. Slodeka, A.; Schnurpfeilb, G.; Wöhrle, D. Optical limiting of germanium(IV) and tin(IV) phthalocyanines in solution and polymer matrices and comparison to an indium(III) phthalocyanine. *J. Porphyr. Phthalocyanines* **2017**, *21*, 811–823. [[CrossRef](#)]
92. Slodek, A.; Wöhrle, D.; Doyle, J.J.; Blau, W. Metal Complexes of Phthalocyanines in Polymers as Suitable Materials for Optical Limiting. *Macromol. Symp.* **2006**, *235*, 9–18. [[CrossRef](#)]
93. Louzada, M.; Britton, J.; Nyokong, T.; Khene, S. Solvent Effect on the Third-Order Nonlinear Optical Properties of  $\alpha$ - and  $\beta$ -Tertbutyl Phenoxy-Substituted Tin(IV) Chloride Phthalocyanines. *J. Phys. Chem. A* **2017**. [[CrossRef](#)]
94. Zhong, A.; Zhang, Y.; Bian, Y. Structures and spectroscopic properties of nonperipherally and peripherally substituted metal-free phthalocyanines: A substitution effect study based on density functional theory calculations. *J. Mol. Graph. Model.* **2010**, *29*, 470–480. [[CrossRef](#)]
95. Li, D.; Hu, R.; Zhou, W.; Sun, P.; Kan, Y.; Tian, Y.; Zhou, H.; Wu, J.; Tao, X.; Jiang, M. Synthesis, Structures, and Photophysical Properties of Two Organostannoxanes from a Novel Acrylic Acid Derived from Phenothiazine. *Eur. J. Inorg. Chem.* **2009**, *2009*, 2664–2672. [[CrossRef](#)]
96. Zhao, X.; Liu, J.; Wang, H.; Zou, Y.; Li, S.; Zhang, S.; Zhou, H.; Wu, J.; Tian, Y. Synthesis, crystal structures and two-photon absorption properties of triphenylamine cyanoacetic acid derivative and its organostannoxane complexes. *Dalton Trans.* **2015**, *44*, 701–709. [[CrossRef](#)] [[PubMed](#)]
97. Wang, H.; Hu, L.; Du, W.; Tian, X.; Zhang, Q.; Hu, Z.; Luo, L.; Zhou, H.; Wu, J.; Tian, Y. Two-Photon Active Organotin(IV) Carboxylate Complexes for Visualization of Anticancer Action. *ACS Biomater. Sci. Eng.* **2017**, *3*, 836–842. [[CrossRef](#)]

98. Guan, R.; Zhou, Z.; Zhang, M.; Liu, H.; Du, W.; Tian, X.; Zhang, Q.; Zhou, H.; Wu, J.; Tian, Y. Organotin(IV) carboxylate complexes containing polyether oxygen chains with two-photon absorption in the near infrared region and their anticancer activity. *Dyes Pigment.* **2018**, *158*, 428–437. [CrossRef]
99. Farfán, N.; Mancilla, T.; Santillan, R.; Gutiérrez, A.; Zamudio-Rivera, L.S.; Beltrán, H.I. Preference of di-n-butyltin(IV) compounds to build O...Sn bonds in fused rings with five-six members. *J. Organomet. Chem.* **2004**, *689*, 3481–3491. [CrossRef]
100. García-Zarracino, R.; Ramos-Quñones, J.; Höpfl, H. Self-Assembly of Dialkyltin(IV) Moieties and Aromatic Dicarboxylates to Complexes with a Polymeric or a Discrete Trinuclear Macrocyclic Structure in the Solid State and a Mixture of Fast Interchanging Cyclooligomeric Structures in Solution. *Inorg. Chem.* **2003**, *42*, 3835–3845. [CrossRef] [PubMed]
101. García-Zarracino, R.; Höpfl, H. A 3D hybrid network containing large spherical cavities formed through a combination of metal coordination and hydrogen bonding. *Angew. Chem. Int. Ed.* **2004**, *43*, 1507–1511. [CrossRef] [PubMed]
102. Zhu, X.; Zheng, L.; Huang, X.; Wu, J.; Hong, L.; Dong, J.; Zhuo, S.; Chen, J. Nonlinear Optical Microscopy Captures High-Resolution Images of Microstructures within Three Types of Unlabeled Rat Cartilage. *IEEE Photonics J.* **2016**, *8*. [CrossRef]
103. Kim, H.M.; Cho, B.R. Small-Molecule Two-Photon Probes for Bioimaging Applications. *Chem. Rev.* **2015**, *115*, 5014–5055. [CrossRef]
104. Helmchen, F.; Denk, W. Deep tissue two-photon microscopy. *Nat. Methods* **2005**, *2*, 932–940. [CrossRef]
105. Zipfel, W.R.; Williams, R.M.; Webb, W.W. Nonlinear magic: Multiphoton microscopy in the biosciences. *Nat. Biotechnol.* **2003**, *21*, 1369–1377. [CrossRef]
106. Myung Kim, H.; Rae Cho, B. Two-photon materials with large two-photon cross sections. Structure–property relationship. *Chem. Commun.* **2009**, 153–164. [CrossRef] [PubMed]
107. Hu, L.; Wang, H.; Xia, T.; Fang, B.; Shen, Y.; Zhang, Q.; Tian, X.; Zhou, H.; Wu, J.; Tian, Y. Two-Photon-Active Organotin(IV) Complexes for Antibacterial Function and Superresolution Bacteria Imaging. *Inorg. Chem.* **2018**, *57*, 6340–6348. [CrossRef] [PubMed]
108. Hu, Y.; Zhang, J.; Li, Z.; Li, T. Crystal structure, Z-scan measurements and theoretical calculations of third-order nonlinear optical properties of tetrachloro(1,10-phenanthroline-*N,N'*)tin(IV). *Synth. Met.* **2014**, *197*, 194–197. [CrossRef]
109. Zugazagoitia, J.S.; Maya, M.; Damiaán-Zea, C.; Navarro, P.; Beltrán, H.I.; Peon, J. Excited-State Dynamics and Two-Photon Absorption Cross Sections of Fluorescent Diphenyl-Tin IV Derivatives with Schiff Bases: A Comparative Study of the Effect of Chelation from the Ultrafast to the Steady-State Time Scale. *J. Phys. Chem. A* **2010**, *114*, 704–714. [CrossRef] [PubMed]
110. García-López, M.C.; Muñoz-Flores, B.M.; Chan-Navarro, R.; Jiménez-Pérez, V.M.; Moggio, I.; Arias, E.; Rodríguez-Ortega, A.; Ochoa, M.E. Microwave-assisted synthesis, third-order nonlinear optical properties, voltammetry cyclic and theoretical calculations of organotin compounds bearing push-pull Schiff bases. *J. Organomet. Chem.* **2016**, *806*, 68–76. [CrossRef]
111. Enríquez-Cabrera, A.; Vega-Peñaloza, A.; Álvarez-Venicio, V.; Romero-Ávila, M.; Lacroix, P.G.; Ramos-Ortiz, G.; Santillan, R.; Farfán, N. Two-photon absorption properties of four new pentacoordinated diorganotin complexes derived from Schiff bases with fluorene. *J. Organomet. Chem.* **2018**, *855*, 51–58. [CrossRef]
112. Morales, A.R.; Frazer, A.; Woodward, A.W.; Ahn-White, H.-Y.; Fonari, A.; Tongwa, P.; Timofeeva, T.; Belfield, K.D. Design, Synthesis, and Structural and Spectroscopic Studies of Push–Pull Two-Photon Absorbing Chromophores with Acceptor Groups of Varying Strength. *J. Org. Chem.* **2013**, *78*, 1014–1025. [CrossRef]
113. Moura, G.L.C.; Simas, A.M. Two-photon absorption by fluorene derivatives: Systematic molecular design. *J. Phys. Chem. C* **2010**, *114*, 6106–6116. [CrossRef]
114. Yao, S.; Ahn, H.Y.; Wang, X.; Fu, J.; Van Stryland, E.W.; Hagan, D.J.; Belfield, K.D. Donor–acceptor–donor fluorene derivatives for two-photon fluorescence lysosomal imaging. *J. Org. Chem.* **2010**, *75*, 3965–3974. [CrossRef]

